

Published in final edited form as:

Tetrahedron. 2011 December 23; 67(51): 9809–9828. doi:10.1016/j.tet.2011.09.035.

(+)-Sorangicin A: evolution of a viable synthetic strategy

Amos B. Smith III^{*}, Shuzhi Dong, Richard J Fox, Jehrod B. Brenneman, John A. Vanecko, and Tomohiro Maegawa

Department of Chemistry, Laboratory for Research on the Structure of Matter, and Monell Chemical Senses Center, University of Pennsylvania, Philadelphia, PA 19104, United States

Abstract

An effective, asymmetric total synthesis of the antibiotic (+)-sorangicin A (**1**) has been achieved. Central to this venture was the development of first and second generation syntheses of the signature dioxabicyclo[3.2.1]octane core, the first featuring chemo- and stereoselective epoxide ring openings facilitated by a $\text{Co}_2(\text{CO})_6$ -alkyne complex, the second involving a KHMDS-promoted epoxide ring formation/opening cascade. Additional highlights include effective construction of the dihydro- and tetrahydropyran ring systems, respectively via a stereoselective conjugate addition/ α -oxygenation protocol and a thioketalization/hydrostannane reduction sequence. Late-stage achievements entailed two Julia–Kociński olefinations to unite three advanced fragments with high *E*-stereoselectivity, followed by a modified Stille protocol to introduce the *Z,Z,E* trienoate moiety, thereby completing the carbon skeleton. Mukaiyama macrolactonization, followed by carefully orchestrated Lewis and protic acid-promoted deprotections that suppressed isomerization and/or destruction of the sensitive (*Z,Z,E*)-trienoate linkage completed the first, and to date only, total synthesis of (+)-sorangicin A (**1**)

Keywords

Sorangicin A; Antibiotic; Trienoate linkage; Julia-Kociński olefination; Total synthesis

1. Introduction

In 1985 Höfle, Jansen, and co-workers reported the isolation and structural elucidation of a new class of macrolide antibiotics termed the sorangicins, from a fermentation broth derived from the myxobacteria *Sorangium cellulosum* (strain So ce 12).¹ Sorangicin A (**1**, Figure 1), the most prevalent and potent congener, displayed extraordinary antibiotic activity against both Gram-positive and Gram-negative bacteria with minimum inhibitory concentrations (MIC) of 0.01–0.3 and 3–25 $\mu\text{g}/\text{mL}$, respectively.

Subsequently the Jansen group demonstrated that the mechanism of action entails inhibition of DNA-dependent RNA polymerase (RNAP) both in *Escherichia coli* (*E. coli*) and *Staphylococcus aureus*, while not affecting eukaryotic cells.² Rats infected with virulent *E.*

© 2011 Elsevier Ltd. All rights reserved.

^{*}Corresponding author. Tel.: +0-000-000-0000; fax: +0-000-000-0000, author@university.edu.

Supplementary Material

Experimental procedures, crystallographic information files, complete spectroscopic and analytical data for new compounds can be found in the online version.

Publisher's Disclaimer: This is a PDF file of an unedited manuscript that has been accepted for publication. As a service to our customers we are providing this early version of the manuscript. The manuscript will undergo copyediting, typesetting, and review of the resulting proof before it is published in its final citable form. Please note that during the production process errors may be discovered which could affect the content, and all legal disclaimers that apply to the journal pertain.

coli underwent marked improvement when dosed with sorangicin A. Comparison studies, in conjunction with the Darst group, of (+)-sorangicin A (**1**) and rifampicin (**2**, Figure 1), the latter a clinically used ansamycin antibiotic possessing a broad spectrum of activity, revealed that, despite being chemically unrelated, the two antibiotics possess remarkably similar overall molecular shapes, leading to the same mechanism of action, namely inhibition of RNA elongation by binding to the same β -subunit pocket of RNAP.³ Importantly, in cross-resistance studies (+)-sorangicin A displayed an advantage against rifampicin-resistant microbial mutants. This observation, based on molecular dynamic simulations, was proposed to arise from an increase in conformational flexibility of the C(14)–C(20) segment of (+)-sorangicin A, permitting better adaptation to mutational changes within the RNAP binding pocket. As such, conformational flexibility of sorangicin A and analogues thereof holds important implications for future drug design against rapidly mutating pathogenic bacteria.³

Architecturally (+)-sorangicin A (**1**) is comprised of a C(1)–C(8) carboxylic acid side chain, attached to a highly unsaturated 31-membered macrocyclic lactone, possessing 15 stereogenic centers. Structural elements inscribed within the macrocyclic ring include the signature dioxabicyclic[3.2.1]octane, a rare (*Z,Z,E*)-trienoate linkage, and di- and tetrahydropyran ring systems. Initially the backbone connectivity, relative stereochemistry and olefin geometries were assigned based on extensive one- and two-dimensional NMR experiments, along with molecular weight assignment by mass spectrometry. X-ray analysis confirmed the structure and stereochemistry, with the absolute configuration being verified via a Hamilton test.⁴ Of interest was the observation of dynamic disorder in the crystalline solid in the C(17)–C(18) region. Significant solvent and pH effects were also observed in the NMR spectra, presumably due to a hydrogen bond between the C(1) carboxyl oxygen and the C(21, 22, and 25)-triol moiety.⁴

In addition to (+)-sorangicin A (**1**), 12 additional sorangicin congeners have been reported, with 8 possessing varying degrees of isomerization of the C(37)–C(43) trienoate region, the latter suggesting instability of this linkage.⁵ That (+)-sorangicin A (**1**) possessed considerable instability leading to decomposition was demonstrated upon treatment with a variety of reagents (e.g., fluoride ion, DDQ, and the dissolving metal sodium amalgam).⁶ Taken together, the intricate and challenging architecture, in conjunction with the potent antibiotic activity, and novel mechanism of action has led to considerable interest in (+)-sorangicin A (**1**) by the synthetic community, including pioneering studies from the Morken,⁷ Schinzer,⁸ Lee,⁹ and Yadav¹⁰ research groups, with a recent (2011) formal total synthesis achieved by Crimmins et. al.¹¹ Herein we provide a full account on the evolution of a synthetic strategy, that in 2009 led to the first, and to date only, total synthesis of this architecturally intriguing antibiotic.¹²

At the outset of this synthetic program, we relied on the structure of (+)-sorangicin A to possess the *R*-configuration at C(10) (Scheme 1, Structure **3**) as depicted in reference 6, and not as originally reported correctly in reference 4 as *S* at C(10) (Figure 1, Structure **1**). As will be described, this misunderstanding came to light late in our synthetic venture (*vide infra*).

2. Results and Discussion

2.1. Initial Synthetic Planning

At the outset of the total synthesis that follows, a central tenet was to take full advantage of the reported chemical sensitivities of (+)-sorangicin A.⁶ Toward this end, we initially planned to mask the delicate (*Z,Z,E*)-trienoate moiety as dienyne (**4**) to attenuate the potential for isomerization and/or decomposition (Scheme 1). Disconnection of **4** at the

macrocyclic lactone, the C(38)–C(39) σ -bond, and both the C(15)–C(16) and C(29)–C(30) *trans* disubstituted olefins revealed four potential advanced subtargets: the signature bicyclic aldehyde **5**, tetrahydropyran **6**, dihydropyran **7**, and enyne **8**. In the forward sense, we envisioned consecutive Julia–Kociński unions of **6** with **5** and **7** to install the C(29)–C(30) and C(15)–C(16) *trans* olefins, thereby uniting three of the four advanced fragments. Subsequent Stille union of known enyne **8**¹³ with the strategically placed C(38) vinyl iodide in **5** was anticipated to complete construction of the full carbon skeleton possessing a dienyne moiety. Macrolactonization and semihydrogenation at a late stage would then be followed by global deprotection to reveal the labile (*Z,Z,E*)-triene. To mask the vicinal 21,22-diol in **6** during construction of the (+)-sorangicin A skeleton, we selected a dimethyl acetonide, since protection and deprotection of (+)-sorangicin A (**1**) employing the acetonide functionality had been successfully achieved by Höfle and co-workers in conjunction with the preparation of various sorangicin analogues.¹⁴ Protection of the C(25) hydroxyl as a MOM ether (illustrated in **6**) and the C(1) carboxylic acid as a *t*-butyl ester (depicted in **7**) were also envisioned, considering their acid lability. Importantly their removal would not require use of fluoride, oxidizing and/or reducing agents, conditions known to destroy the natural product.

Continuing with this analysis, the signature 2,6-dioxabicyclo[3.2.1]octane was anticipated to arise via an unprecedented chemo- and stereoselective epoxide ring-opening cascade of **9**, facilitated by a Co₂(CO)₆-alkyne complex (Scheme 2). That is, upon formation of the Co₂(CO)₆-alkyne complex of bis-epoxide **10**, a stereocontrolled epoxide ring-opening of the activated propargylic epoxide mediated by acid would generate the tetrahydrofuran ring; completion of the bicyclic skeleton would then entail a 6-exotet epoxide ring-opening via the derived C(35) secondary hydroxyl. For construction of sulfone **6**, the presence of the 2,6-*cis*-disubstituted tetrahydropyran ring initially suggested application of the Petasis–Ferrier union/rearrangement protocol, a tactic developed in our laboratory,¹⁵ which would unite known β -hydroxy acid (+)-**11**^{15d} with aldehyde (+)-**12**.¹⁶ Finally, construction of 2,3,6-*trans*, *cis*-trisubstituted dihydropyran **7** would call upon conjugate addition of vinyl bromide **14** to known dihydropyranone (–)-**13**,¹⁷ followed by α -oxygenation and elaboration of the C(11,12) double bond. Stereocontrol during construction of **7** would be provided by the stereogenicity at C(13) (Scheme 2).

2.2. Construction of the Signature Dioxabicyclo[3.2.1]octane Fragment 5 (Figure 2): Application of a Cyclization Cascade Facilitated by a Co₂(CO)₆-Acetylene Complex

In 1994, Mukai and co-workers introduced stereocomplementary approaches to *cis*- and *trans*-2-ethynyl-3-hydroxytetrahydrofurans via epoxide ring-opening of 3,4-epoxy-6-substituted hex-5-yn-1-ols (Scheme 3).¹⁸ Specifically, exposure of either the *trans*- or *cis*-epoxy alcohol (**15** or **16**) to BF₃•OEt₂ resulted in intramolecular epoxide ring-opening with *inversion* of stereogenicity at the propargylic center to furnish respectively the *trans*- or *cis*-tetrahydrofurans (i.e., **15** → **17**, or **16** → **18**). Alternatively, addition of BF₃•OEt₂ to the corresponding Co₂(CO)₆-alkyne complexes induced “Nicholas” cyclizations¹⁹ to furnish respectively the *cis*- or *trans*-cobalt-complexed tetrahydrofurans. Importantly, epoxide ring-opening proceeded with overall *retention* of stereochemistry at the propargylic center. Subsequent demetallation with ceric ammonium nitrate (CAN) led to the respective tetrahydrofuran in a single-flask (i.e., **15** → **18**, or **16** → **17**). The observed retention of stereochemistry **7** for the epoxide ring-opening was rationalized to involve a double-S_NII inversion.²⁰

Based on this precedent, we became intrigued with the feasibility of constructing the (+)-sorangicin A signature bicycle subunit beginning with bis-epoxide **10** exploiting a four-step, one-flask reaction sequence (Scheme 4). If successful, a very rapid, highly stereocontrolled route to the signature subunit of (+)-sorangicin A would be in hand.

Our synthetic analysis of bis-epoxide **10** (Scheme 5) thus began with removal of both epoxides, and in turn scission of the C(34)–C(35) σ -bond to afford epoxy alcohol **23** and known vinyl bromide **24**.²¹ In the forward sense, we envisioned that epoxide ring-opening of **23** via an organometallic reagent derived from **24** would furnish enyne **22**; removal of the PMB group, ring-closure to furnish the terminal epoxide, and application of the elegant Shi oxidation protocol would provide bis-epoxide **10**, the substrate for the proposed four-step construction of **21**. Continuing with this analysis, removal of the epoxide moiety in **23** leads to a homoallylic alcohol,²² which upon application of a Brown crotylation retron, yields known aldehyde **25**.²³

We began the synthesis of **21** with aldehyde **25**. Initially, bis-PMB ether **26**,²⁴ prepared from *cis*-2-butene-1,4-diol, was subjected to ozonolysis, in the presence of Sudan III as indicator,²⁵ followed by reductive workup (PPh₃). Kugelrohr distillation reproducibly furnished aldehyde **25** in 53% yield (Scheme 6). On larger scale (ca. 35 g), yields however were variable. As an alternative, ozonolysis of **26**, followed by reduction of the ozonide, recrystallization and basic extractive workup of the derived bisulfite adduct **27**²⁶ provided aldehyde **25** on 35 g scale in 69% yield (3 steps) from *cis*-2-butene-1,4-diol, without chromatography or distillation.

Brown crotylation,²⁷ followed by Sharpless dihydroxylation,²⁸ next furnished triol (+)-**29** in 74% yield for the two steps as a separable mixture (9:1) of diastereomers (Scheme 7). The absolute configuration of (+)-**28** was confirmed via Mosher ester analysis, exploiting the Kakisawa test,²⁹ while the relative stereochemistry of the major diastereomer [(+)-**29**], obtained via Sharpless dihydroxylation, was verified via the Rychnovsky-Evans empirical ¹³C acetonide tactic.³⁰ Application of the Fraser-Reid epoxide ring construction furnished epoxide (+)-**23** in modest yield (42–44%), after separation of the minor diastereomer, along with 15–16% trisylated product (–)-**30**.³¹ To eliminate over-trisylation, 1.05 equivalents of KHMDS could be used, employing slow addition of the trisylimid (1.5 h) as reported by Forsyth and coworkers.³² Although these conditions eliminated over trisylation, the yield of (+)-**23** remained modest (48%).

With a route, albeit non-optimal, to epoxide (+)-**23** established, we turned to union with **24** (Scheme 8). To our dismay, efforts to prepare the vinyl Grignard derived from **24**,²¹ followed by addition to epoxide (+)-**23**, led only to recovery of starting materials.³³

We therefore turned to installation of the *E*-enyne moiety via the anion derived from commercially available 1,4-bis(trimethylsilyl)-1,3-butadiyne (**33**) (Scheme 9),³⁴ followed by chemo- and stereoselective reduction of the internal triple bond, directed by the resulting homoallylic alcohol.³⁵ However to proceed with this scenario, improvement of the low efficiency of the conversion of triol (+)-**29** to epoxide (+)-**23** was required (i.e., 48% yield, Scheme 7). The hydroxyl group in (+)-**28** was therefore protected as a PMB ether with the view of circumventing potential over-trisylation in the epoxide ring-closure. Sharpless dihydroxylation²⁸ followed by application of the Fraser-Reid protocol³¹ then led to epoxide (–)-**32** in excellent yield (98%) as a single diastereomer (Scheme 9).

With ample quantities of epoxide (–)-**32** in hand, we examined the ring-opening with lithium trimethylsilylbutadiyne.³⁶ Pleasingly generation of lithium trimethylsilylbutadiyne (2 equiv), followed by inverse addition of epoxide (–)-**32** in THF containing BF₃•OEt₂ furnished alcohol (–)-**34** in 92% yield on a 20 g scale (Scheme 9). Pre-cooling the THF/BF₃•OEt₂ solution of epoxide (–)-**32** to –78 °C, prior to addition to the –78 °C THF solution of lithium trimethylsilylbutadiyne, and executing an inverse reaction quench with NH₄Cl (Sat.) proved critical to achieving a high yield of (–)-**34**. Reduction with LiAlH₄, followed by oxidative removal of both PMB groups furnished in turn alcohol (–)-**35** and

triol (+)-**36**, both in excellent yield as single *E*-isomers.³⁵ Presumably, the chemo- and *E*-stereoselectivity arises via generation of an alkenyl aluminate (i.e., **37**).^{37,38}

What remained to complete the synthesis of bis-epoxide **10** was to form the internal and terminal epoxides. Unfortunately, closure of triol (+)-**36** to terminal epoxide (+)-**38** led irreproducibly to (+)-**38** under a variety of conditions (Scheme 10A). Alternatively, protection of (–)-**35** as the *tert*-butyl-diphenylsilyl (BPS) ether (Scheme 10B), followed by oxidative removal of both PMB groups and epoxide formation, employing the Mitsunobu conditions, reproducibly furnished terminal epoxide (–)-**39** in 66% yield (three steps on a 4 g scale).

Initially the critical Shi epoxidation³⁹ of alcohol (+)-**38** led to (+)-**10** with modest efficiency (Scheme 11). Better results were obtained with (–)-**39**, when the oxidation was carried out at low concentration (0.016 M) with addition of oxone and K₂CO₃ over 5 h; bis-epoxide (–)-**40** was reproducibly formed in 66% yield, along with 22% recovered starting material.

Our goal, with bis-epoxides (+)-**10** and (–)-**40** now available, was to construct the signature 2,6-dioxabicyclo[3.2.1]octane ring system of (+)-sorangicin A in a single-flask via the proposed sequential bis-epoxide ring-opening cascade (see Scheme 4). To define the landscape of this cyclization process, we initially investigated a stepwise protocol. Treatment of bis-epoxide (+)-**10** with 1.1 equiv Co₂(CO)₈ in CH₂Cl₂ at ambient temperature, followed by 0.10 equiv BF₃•OEt₂ at –78 °C, furnished cobalt complex (+)-**19** in 75% yield as a single *cis*-isomer (Scheme 12). Pleasingly, the reaction proceeded with complete chemoselectivity at the activated propargylic epoxide. Single-crystal X-ray analysis verified that the epoxide opening had occurred with retention of stereochemistry.¹⁸

Turning to the second epoxide-ring opening in the same flask, treatment of (+)-**19** with a variety of acids and bases failed to produce the desired bicycle **20** (Scheme 12). Instead, selective formation of bicycle (–)-**41**, arising from a 7-endo-tet cyclization, was observed with camphorsulfuric acid (CSA), while with BF₃•OEt₂, mixtures of (–)-**41**, along with respectively 6- and 7-membered bicycles (–)-**42** and (–)-**43** were formed, both having undergone epimerization (!) at the propargylic center. The structure and stereochemistry of bicycles (–)-**41**, (–)-**42** and (–)-**43** were assigned via ¹H, COSY and D₂O exchange experiments. Reexposure of the individual bicycles to BF₃•OEt₂ did not result in any improvement, suggesting that the cyclizations proceeded via kinetic control.

Based on the X-ray crystal structure of (+)-**19** (Scheme 12), we reasoned that the steric bulk of the cobalt complex disfavored the desired 6-exo-tet ring-opening process, thereby preventing a one-flask cascade. We therefore removed the cobalt moiety from the alkyne prior to attempting the second cyclization (Scheme 13). A three-step operation, performed in a single-flask, furnished epoxide (–)-**44** in 88% yield.

Reducing the steric bulk of alkyne did indeed facilitate the 6-exo-tet pathway, furnishing the desired bicycle (–)-**21**, upon treatment of epoxide (–)-**44** with 0.10 equiv CSA in CH₂Cl₂ at ambient temperature. An equal amount of the undesired 7-endo-tet bicycle (–)-**45** was also formed (Table 1, Entry 1). Importantly, no epimerized products were observed. Employing BF₃•OEt₂ at higher temperatures increased both the reaction rate and the amount of the desired 6-exo-tet bicycle (compare Entries 2 and 3; 5 and 6). Best results were obtained with 0.1 eq BF₃•OEt₂ at 40 °C to afford a 1:1 ratio of (–)-**21** and (–)-**45** (Entry 4). Attempts to increase the yield of (–)-**21** with other Lewis acids (e.g., TiCl₄ or CeCl₃), or under basic conditions (e.g., KH, DMSO) proved unsuccessful.⁴⁰

Having achieved access to bicycle (–)-**21**, we envisioned further enhancing the ratio of the 6-exo-tet derived bicycle by additional reduction of steric bulk at the alkyne. Accordingly,

the TMS group of (–)-**44** was removed to furnish (–)-**46**. Conditions identical to those employed in Entry 3 (Table 1) did modestly enhance delivery of the desired tricycle (–)-**47** (1.4:1, Entry 1, Table 2). Single crystal X-ray analyses verified the structures and stereochemistries of both (–)-**47** and (–)-**48**. We next performed the cyclization by addition of (–)-**46** to a solution of CH₂Cl₂ at reflux for 5 minutes, containing 10.0 equiv BF₃•OEt₂. Again modest improvement in the product ratio (ca. 2.1:1) was achieved (Entry 2). Solvents such as benzene or acetonitrile at a variety of temperatures however led to no improvement. Notably, uncatalyzed bicycle formation was observed upon storing neat (–)-**46** at –20 °C, favoring the undesired 7-endo-tet product (1:2, Entry 6).

We also explored a series of acids, stronger than BF₃•OEt₂ (Table 2). The best ratio of desired to undesired bicycle was achieved with TfOH (2.5:1, Entry 3), however the BF₃•OEt₂ conditions (Entry 2) provided a higher overall yield (65%) of (–)-**47**. The conditions in Entry 2 were therefore employed to advance material to (–)-**47**.

Having achieved construction of bicycle (–)-**47**, we were of course cognizant that preparation and epoxidation of enyne (+)-**38** was less efficient than the synthesis and epoxidation of BPS-protected enyne (–)-**39** (see Schemes 10 and 11). For material advancement, we therefore utilized the BPS-protected bis-epoxide (–)-**40** to furnish (–)-**47** in gram quantities (Scheme 14).⁴¹

Completion of the synthesis of (–)-**5**, the signature core fragment for (+)-sorangicin A (**1**), was achieved via radical induced hydrostannylation/iodination⁴² of (–)-**47**, followed by Dess-Martin oxidation.⁴³ Interestingly, application of a palladium-catalyzed hydrostannylation protocol,⁴⁴ followed by iodination, furnished the undesired α -iodide as the major regioisomer, while use of iodine in place of NIS in the AIBN promoted hydrostannylation led to significant protodestannylation, presumably due to the formation of HI upon addition of iodine to the excess Bu₃SnH. In the end, the signature core fragment (–)-**5** for (+)-sorangicin A could be prepared in 15 steps (longest linear sequence) and in 3% overall yield utilizing the Co₂(CO)₆-alkyne complex approach.^{12a}

2.3. A Second-Generation Synthesis of the Bicycle (–)-**5**: Development of a KHMDS-Promoted Cyclization Cascade

Although effective, the first-generation synthesis of (–)-**5** was not considered sufficiently efficient vis-à-vis material advancement; a second generation approach based on precedence from the Crimmins laboratory^{11a} was therefore developed. Early on we had recognized that the pyran portion of bicyclic aldehyde (–)-**5** shares the same 2,6-*trans*-relationship as dihydropyran **7** (Scheme 1). We therefore envisioned a route featuring a similar substrate-controlled, stereoselective conjugate addition of a Michael donor to dihydropyranone (–)-**13** (*vide infra*), followed by electrophilic trapping to install the C(47) methyl group (Scheme 15). In retrospect, the synthesis of (+)-sorangicin A would be significantly streamlined if two of the major subtargets would arise from the same homochiral starting material. The second-generation route would also be differentiated from the Co₂(CO)₆-alkyne approach by constructing the tetrahydropyran ring in advance of the tetrahydrofuran moiety, a tactic that was envisioned to avoid the 7-endo-tet cyclization.

Construction of dihydropyranone (–)-**13**⁴⁵ began by exploiting a hetero Diels-Alder (HDA) reaction between the Danishefsky diene⁴⁶ and aldehyde **51**,⁴⁷ promoted by chromium(III) complex **52**⁴⁸ (Scheme 16). Both the yield and enantioselectivity proved excellent (98%; 20:1 e.r.). A three-component conjugate addition/alkylation sequence involving dihydropyranone (–)-**13**, a suitable Michael donor, disguised as an aldehyde synthon, and methyl iodide, were employed to fashion the requisite 2,3,6-*trans*, *cis*-configuration. Initially, dihydropyranone (–)-**13** was expected to be a somewhat reluctant Michael

acceptor, as the ring oxygen would deactivate the β position.⁴⁹ Indeed, efforts to add a mixed zincate, derived from $\text{BnOCH}_2\text{SnBu}_3$, resulted only in recovery of the starting enone, even with promoters such as $\text{Cu}(\text{OTf})_2$ and $\text{P}(\text{OEt})_3$.⁵⁰ These observations however proved to be more of a donor problem, as α -alkoxycopper reagents lack reactivity toward Michael additions.⁵¹

Recourse was thus made to the commercially available β -bromostyrene (**53**), a surrogate addend, with a view to achieving oxidative cleavage of the styrene olefin at a later stage (Scheme 17). Pleasingly, the mixed zincate, generated via lithiation of β -bromostyrene (**53**) and transmetalation with Me_2Zn , underwent effective conjugate addition to dihydropyranone (–)-**13** to furnish the zinc enolate, which upon quenching with excess MeI and HMPA furnished adduct **54** (62%).⁵² Although commercial β -bromostyrene is a *cis/trans* isomeric mixture (ca. 1:9), **54** was obtained as a single diastereomer (confirmed by *nOe* studies), the result of excellent substrate control, as well as low reactivity of the minor *cis*-derived zincate.⁵³

Reduction of tetrahydropyranone **54** with L-Selectride then furnished a single diastereomer; again the newly generated stereogenic center was verified via *nOe* correlations. Protection of the secondary hydroxyl **55** was next envisioned, followed by desilylation and Grieco elimination to furnish diene **56**, which was projected to undergo stereoselective dihydroxylation to furnish diol **57**. Attack by the C(33) hydroxyl that proceeds with inversion of the C(36) stereogenicity would be required to construct the bicyclic skeleton possessing the *S* configuration at C(36). A critical question remained: could the requisite chemoselective oxidation of the terminal alkene be achieved in the presence of the electron rich styrene olefin?

With this issue in mind, further analysis revealed that the synthesis of subtarget (–)-**5** could be significantly streamlined if the *S*-configuration at C(36) was installed early on. Dihydropyranone (–)-**59**⁵⁴ (Scheme 18) was therefore selected as a more advanced Michael acceptor, possessing the *S*-configuration at C(36). Pleasingly, this Michael acceptor could be readily prepared via cyclocondensation between the Danishefsky diene⁴⁶ and aldehyde (–)-**58**,⁵⁵ employing the same Jacobsen catalyst **52**.⁴⁸ An analogous three-component coupling protocol furnished adduct (+)-**61** (51%), again as a single diastereomer via Zn-enolate **60**. Careful examination of the reaction mixture, however, led to the isolation and identification of α,α' -bismethylated product (+)-**62** (ca. 20%). The mechanism of this side reaction is ascribed to the unusual reactivity of Zn-enolate **60**; a similar observation was recorded by Alexakis et al.⁵⁶ The heightened reactivity of the Zn-enolate (**60**) could be mitigated by addition of $\text{CuI}\cdot\text{PBU}_3$ just prior to the addition of MeI . The result was a slower, albeit effective reaction process furnishing (+)-**61** in 73% yield. Other copper species, including $\text{Cu}(\text{OTf})_2\cdot\text{P}(\text{OEt})_3$ and (2-Th) $\text{Cu}(\text{CN})\text{Li}$, also proved effective.

Having assembled (+)-**61** in two steps, L-Selectride reduction followed by acid promoted deprotection led to triol (–)-**63**, setting the stage for the critical tetrahydrofuran ring construction (Scheme 19).

Regioselective sulfonylation of the least hindered hydroxyl in (–)-**63** was readily achieved with KHMDS (1 equiv), followed by the slow addition of the bulky Trisylimid (1 equiv), which in turn was treated with an additional 2 equiv KHMDS to promote the expected cyclization cascade, involving epoxide ring formation followed by epoxide opening to generate bicycle (–)-**66**.³² The yield of (–)-**66** however was disappointing (33%); the major side product proved to be over-sulfonylation to furnish (–)-**67** (36%). Lowering the reaction temperature or use of potassium *tert*-butoxide in *tert*-butanol³² did not affect an improvement. We therefore turned to an alternative stepwise protocol developed by the

Tanaka group.⁵⁷ Treatment of (–)-**63** with triisopropyl-benzenesulfonyl chloride (TrisylCl) in pyridine/CH₂Cl₂ at room temperature (Scheme 20) selectively furnished the primary sulfonate (–)-**68** in 77% yield, which proved stable to regular laboratory handling. Addition of 1.2 equiv KHMDS then delivered (–)-**66** in excellent yield (91%). Thus, the signature dioxabicyclo[3.2.1]octane core of (+)-sorangicin A (**1**) could now be elaborated in 6 steps and 35% overall yield from (–)-**58**.

To arrive at advanced bicycle (–)-**5** (Scheme 20), installation of the *trans* vinyl iodide and access to the C(30) aldehyde remained. Toward this end, (–)-**66** was subjected to Parikh-Doering oxidation,⁵⁸ and without purification, the resultant sensitive aldehyde subjected immediately to Takai olefination conditions.⁵⁹ To our surprise, a diastereomeric mixture of *Z/E* isomers (1:3.2) was obtained as evidenced by the observed ¹H NMR olefin coupling constants (8 Hz and 15.8 Hz). This selectivity was contrary to the general trend, in which α -alkoxy-aldehydes are reported to furnish nearly complete *E*-selectivity in the Takai olefination.⁶⁰ Switching the reaction medium from THF to dioxane/THF⁶¹ did not alter the *E/Z* ratio, but did improve the scalability of the process; under these conditions (–)-**69** and (–)-**70** could be obtained in 16% and 52% yield on half gram scale after flash chromatography.

The challenge at this stage was to differentiate the two olefins in (–)-**70**. From the outset we speculated that the vinyl substituents, an electron-withdrawing iodide and an electron-donating phenyl group, might introduce sufficient differences in electron-density to permit the required chemoselectivity. In the event, Sharpless dihydroxylation²⁸ led only to reaction at the styrene olefin in (–)-**70** to furnish the corresponding diol, which upon NaIO₄ treatment with pH 7 buffer generated the desired advanced aldehyde (–)-**5**, now available in 10 steps and 11% overall yield from (–)-**58**.^{12c}

2.4. Construction of Advanced Linchpin Fragment 6

As noted earlier, the 2,6-*cis*-disubstituted tetrahydropyran embedded in fragment **6** (Figure 3) suggested application of the Petasis-Ferrier union/rearrangement tactic, ideally exploiting known β -hydroxy acid (+)-**11**^{15d} and aldehyde (+)-**12**¹⁶ (Scheme 21). This strategy, however, was not without risk. First, the Petasis-Ferrier rearrangement had not previously been employed with either an α -oxygenated aldehyde or a resident acetonide moiety on the aldehyde. Second, there were no examples in a tetrahydro-pyranone endowed with a 2,3,6-*cis*-trisubstitution substituent pattern of selective reduction of a C(4) carbonyl to the corresponding axial alcohol (*vide infra*).

With this overview, we prepared known β -hydroxy acid (+)-**11**^{15d} and aldehyde (+)-**12**,¹⁶ and examined the union/rearrangement tactic. Silylation of (+)-**11**, followed by condensation with (+)-**12**, promoted by TMSOTf,⁶² furnished dioxanone (+)-**71**; Petasis-Tebbe olefination⁶³ then provided enol ether (+)-**72** in 79% yield over the three steps without purification (Scheme 21). Exposure of (+)-**72** to our optimized Lewis acid (Me₂AlCl) protocol, to trigger the Petasis-Ferrier rearrangement, pleasingly furnished tetrahydropyranone (+)-**73** in 70% yield as a single diastereomer. The *cis* stereochemistry was established based on nOe enhancements between H(23) and H(27). This transformation represented the first validated example of an α -oxygenated aldehyde in a Petasis-Ferrier union/rearrangement sequence.⁶⁴

Reduction of the ketone in (+)-**73** to the requisite C(25) axial alcohol however proved to be a major road block. A wide variety of reducing conditions, including K- and L-Selectride, NaBH₄/CeCl₃, the CBS reagents, the latter employing either the (*R*) and (*S*) enantiomers, delivered only the undesired C(25) equatorial alcohol as the major product. Best results were obtained with DIBAL-H, albeit a mixture (1:1) of diastereomers resulted. Equally daunting,

Mitsunobu inversion of the undesired diastereomer led only to elimination. At the time that these results were recorded, a nearly identical observation, including Mitsunobu elimination, was reported by Funk and Cossey⁶⁵ for an analogous 2,3,6-*cis-cis*-trisubstituted tetrahydropyranone. More recently, Yadav and co-workers^{10a} corroborated both observations in their synthesis of an advanced THP fragment for (+)-sorangicin A.

Although we were able to arrive at the required 2,3,6-*cis,cis*-trisubstituted tetrahydropyranone system employing the Petasis-Ferrier union/rearrangement tactic, advancing materials through a sequence involving an unselective tetrahydropyranone reduction was viewed as less than optimal. A second-generation strategy was therefore developed.

2.5. Linchpin 6: A Second-Generation Synthesis

At this stage, we opted to explore a strategy that would first construct a linear precursor for the tetrahydropyran ring system **6**, that would permit installation of the C(25) hydroxyl group with the requisite stereogenicity prior to ring formation (Scheme 22). An aldol tactic between aldehyde **78** and methyl ketone **79** became our focus (Scheme 22). Cyclization of **77** to ketal **75**, followed in turn by reductive deoxygenation, application of a Suzuki–Miyaura union with alkyl boronate **76**, and installation of the phenyltetrazolyl-sulfone (PT) would deliver the required advanced THP fragment **6** after protecting group adjustments. Installation of the C(25) hydroxyl in a stereoselective fashion to furnish **77** was viewed as the principle issue. Boron-mediated aldol reactions involving methyl ketones, governed respectively by the α - or β -alkoxy substituent of the methyl ketone, are known to give rise to the 1,4-*anti* or 1,5-*anti* adducts.⁶⁶ For ketone **79** however the α - and β -benzyloxy groups would operate in an opposite sense. Which structural feature would dominate however was not clear.

With this question in mind, we constructed coupling partners **78** and **79**. Protection of known alcohol (+)-**80**^{15d} as the TES ether, followed by removal of the chiral auxiliary and oxidation with $\text{SO}_3 \cdot \text{py}$ ⁵⁸ furnished aldehyde (+)-**78** in 91% yield over the three steps (Scheme 23A). Methyl ketone **79** was next prepared in five steps (Scheme 23B). Reduction of known lactone (+)-**81**⁶⁷ with DIBAL-H followed by exposure of the resulting lactol to $\text{TMSCHN}_2/\text{LDA}$ ⁶⁸ provided alkynyl alcohol (+)-**82** in good overall yield (85%, 2 steps). Parikh-Doering oxidation⁵⁸ was then followed by methylation of the resulting aldehyde with AlMe_3 ; a second Parikh-Doering oxidation led to the corresponding methyl ketone, albeit with partial racemization at the α -stereogenic center during the methylation. The less basic nucleophile generated from MeMgBr and anhydrous CeCl_3 furnished a pair of diastereomeric secondary alcohols without epimerization. Oxidation then led to methyl ketone (+)-**79** in 74% yield. Overall, the five-step sequence to (+)-**79** proceeded in 62% yield.

With both coupling partners in hand, reaction of aldehyde (+)-**78** (Scheme 24) with the boron enolate derived from methyl ketone (+)-**79** via dicyclohexylboron chloride (Chx_2BCl) led to a separable mixture of C(25) diastereomers (3.2:1), in favor of the desired β -alcohol, demonstrating that in this case, when the α - and β -alkoxy substituents act in opposite fashion, 1,4-*anti* selectivity dominates over 1,5-*anti* selectivity. Treatment of the alcohol mixture with $\text{PPh}_3 \cdot \text{HBr}$ in MeOH to effect desilylation followed by cyclization furnished both (+)-**75**, the desired methyl ketal, and the C(25) epimer (+)-**83** in good yield. Although the aldol diastereoselectivity had proven to be only modest (3.2:1), this route held considerable appeal since the undesired methyl ketal (+)-**83** could be oxidized to tetrahydropyranone (+)-**84**, and then reduced with L-Selectride to deliver (+)-**75** as a single diastereomer (89% yield, 2 steps), permitting advancement of all synthetic material. The difference in stereochemical outcome vis-à-vis the selectivity observed with reductions of

(+)-**73** and (+)-**84** is illustrated in Figure 4. In the case of tetrahydropyranone (+)-**73**, axial attack of the hydride is generally favored, aided by the steric hindrance of the C(26) axial methyl group. In ketone (+)-**84**, the axial trajectory however is highly disfavored due to the axial C(23) methoxy group, leading instead to the desired α -alcohol (+)-**75**.

Synthesis of linchpin **6** continued via reductive deoxygenation of the methyl ketal in (+)-**75**, with Et₃SiH and TMSOTf, followed by MOM protection to furnish tetrahydropyran (+)-**85** in 93% yield for the two steps (Scheme 25). The stereochemical outcome in (+)-**85** was verified by nOe correlations. Installation of the *trans* vinyl iodide moiety was next achieved via a hydrozirconation/iodination protocol,⁶⁹ which in turn permitted Suzuki–Miyaura cross coupling⁷⁰ with alkyl boronate **76**⁷¹ to provide olefin (+)-**86** as a single *E*-isomer, possessing the full carbon skeleton of THP fragment **6**. Debenzylation via treatment with lithium 4,4'-*tert*-butylbiphenolide (LiDBB), followed by acetonide formation and selective removal of the primary BPS group with KOH/DMPU⁷² in acetonitrile then furnished alcohol (+)-**87** in 59% yield for the three steps. The phenyltetrazolyl sulfone (PT) was next installed to arrive at fragment (–)-**6**. Overall (–)-**6** was constructed in 17 steps beginning with commercially available D-erythrone.^{12b}

2.6. An Augmented Synthesis of Advanced Linchpin (–)-**6**

Upon scaling the first-generation synthesis of (–)-**6**, a number of issues were encountered. First, the C(25) axial hydroxy in (+)-**75** was prone to elimination during the Lewis acid promoted reductive deoxygenation. To solve the issue, we envisioned that thioketalization would provide an intermediate that could be reduced under conditions that would not activate the C(25) hydroxyl toward elimination (e.g., radical reduction). A second issue related to removal of the primary BPS-ether in the presence of the primary TBS-ether to afford (+)-**87** employing strong basic conditions. An orthogonal protecting group strategy would address this problem. Aldehyde (+)-**89** (Scheme 26A) possessing a terminal benzyl ether, was therefore prepared from known amide (+)-**88**⁷³ in 2 steps (80%).

To improve convergency, we also decided to introduce the vinyl iodide moiety at an earlier stage. After a number of experiments, hydrozirconation of **90**, protected as the TES ether, (Scheme 26B) with the Schwartz reagent [Cp₂Zr(H)Cl]⁶⁹ and I₂, furnished vinyl iodide **91** in 59% yield along with alkene **92** (12%). Speculating that the Schwartz reagent was reacting to generate HI with the excess iodine, which in turn would quench the intermediate vinylzirconocene to generate **92**, NIS was employed to remove zirconium. These conditions furnished vinyl iodide (+)-**93** in 65% yield along with concomitant desilylation. This sequence could be further streamlined by conducting the hydrozirconation directly on alcohol (+)-**82**, employing LiEt₃BH to achieve deprotonation prior to treatment with the *in situ* generated Schwartz reagent.⁶⁹ These conditions produced (+)-**93** in 87% yield. The resulting vinyl iodide was then converted to methyl ketone (+)-**94** in similar fashion to the conversion of (+)-**82** to (+)-**79** (see Scheme 23).

With both coupling partners in hand, realization of the aldol condensation became our focus. Initial NMR experiments in CD₂Cl₂ indicated that the previously employed Lewis acid Chx₂BCl did not efficiently generate the desired enol-boronate. Consequently, the more reactive Lewis acid, Chx₂BBr,⁷⁴ was employed. Moderate diastereoselectivity (β : α = 3:1) was obtained using a slight excess of the Lewis acid (1.25 equiv), albeit at the expense of yield (33%, Scheme 27). The reaction could be driven to completion by increasing the amount of Lewis acid (3.5 equiv), albeit nearly equal quantities of the α - and β -adducts were obtained, which fortunately could be separated by flash chromatography. The observed modest diastereoselectivity is in line with the expectation that the substituents on (+)-**94** act in the opposite sense to direct the *anti*-selective aldol (*vide ante*). Given that the undesired α -diastereomer was also a viable intermediate, via an oxidation/reduction sequence en route to

sulfone (–)-**6**, further optimization of the aldol reaction was not pursued. Rather both acyclic precursors were utilized in the subsequent thioketalization studies.

Beginning with adduct (+)-**95β**, desilylation was successfully achieved with Et₃N•3HF giving rise to **96**, which exists as a mixture of hemiketal tautomers **96/97** (Scheme 28A). Treatment with a catalytic amount of BF₃•OEt₂ (0.33 equiv) in CH₂Cl₂/EtSH at –15 °C effected thioketalization to produce the desired thioketal (+)-**98** (33%), along with competitive elimination of the C(25) hydroxyl to afford near equal quantities of (+)-**99** (34%). Attempts with different temperature and Lewis acids régimes did not improve the matter. Diastereomer (+)-**95α** fared better under the same thioketalization conditions, resulting in less dehydration and in higher efficiency (Scheme 28B). This was not surprising considering that the equatorial C(25) hydroxyl group in (+)-**102**, based on stereoelectronic effects, would be expected to be less prone to elimination as compared to the C(25) axial diastereomer (+)-**98**.

Gratifyingly, a further screen of solvents with additional optimization revealed that slow addition of a catalytic amount of BF₃•OEt₂ (0.08–0.16 equiv) in MeCN via syringe pump to solutions of both **96** and **100** in MeCN/EtSH furnished the desired thioketals in 82–83% yield, with <10% of dehydration product (+)-**99** observed (Scheme 29).⁷⁵ A similar two-step oxidation/reduction protocol (see Scheme 24) then transformed thioketal (+)-**102** into the desired (+)-**98** with good overall efficiency (83% yield, 2 steps).

At this point, attempts to protect the C(25) hydroxyl of (+)-**98** as the corresponding MOM-ether led only to recovered starting material, suggesting that in the presence of the axial thioethyl group the same steric factor permitting effective conversion of (+)-**102** to (+)-**98** hinders ether formation. Fortunately, extension of the side-chain of (+)-**98** without protection of the C(25)-hydroxyl could be achieved via Suzuki union⁷⁰ with boronate **76**, to furnish (+)-**103** in good yield (85%, Scheme 30).

Initial experiments to reduce the thioketal employing excess Bu₃SnH as the radical reductant provided the desired (+)-**105**, albeit in low yield (ca. 21–28%, Scheme 30). As anticipated the reaction was not plagued by C(25) hydroxyl elimination, however competitive deprotection of the primary benzyl ether occurred, leading to (+)-**104**; yields ranged from 34–52%. Attempts to reprotect the free 1°-hydroxyl as a benzyl ether in the presence of the secondary alcohol were not rewarding.

We reasoned that if the highly reactive tributyltin radicals were responsible for removal of the primary benzyl ether, a less reactive and hence more stable radical source might suppress the debenzylolation process. To this end, we turned to Ph₃SnH to furnish (+)-**105** in 65% yield, with only modest loss of the benzyl group (15%, Scheme 31).

With the axial thioethyl group removed, the C(25) hydroxyl of (+)-**105** was protected as the MOM ether, and in turn, triol (+)-**106** was generated upon treatment with excess lithium 4,4'-di-*tert*-butylbiphenylide (LiDBB) (Scheme 31). Selective conversion of the primary alcohol to the corresponding mesylate (+)-**107** (80%) was then achieved using carefully defined conditions (MsCl, collidine) to avoid loss of the TBS group. The resultant vicinal diol in (+)-**107** was then protected as the acetonide, using 2-methoxypropene and catalytic PPTS, to furnish (+)-**108** in near quantitative yield.

Installation of the Julia-Kociński sulfone, was next achieved via displacement of the mesylate in (+)-**108** with cesium arylthiolate derived from phenyltetrazole-thiol (PTSH) and Cs₂CO₃ in DMF to produce (–)-**109** (97%). Use of the more readily available sodium thiolate on the other hand led to significant β-elimination to furnish the terminal olefin. The Julia-Kociński sulfone (–)-**6** was then generated in excellent yield (96%) upon oxidation

with the ammonium molybdate-hydrogen peroxide oxidative system $[(\text{NH}_4)_6\text{Mo}_7\text{O}_{24}\cdot 4\text{H}_2\text{O}\cdot \text{H}_2\text{O}_2]$.⁷⁶ Overall the thioketalization-based approach produced the requisite advanced THP linchpin (–)-**6** in 17 steps (longest linear sequence) and in 9.2% overall yield.

2.7. Construction of Advanced Dihydropyran Fragment 7 (Figure 5)

As earlier illustrated (Scheme 2), disconnection of the C(8)–C(9) $\text{sp}^2\text{-sp}^3$ carbon-carbon bond in **7** revealed dihydropyranone (–)-**13**¹⁷ and vinyl bromide **14** (Scheme 32). In the synthetic direction, we envisioned that the C(13) stereocenter in (–)-**13** would permit control of the stereochemical outcome at both C(9) and C(10). To this end, 1,4-conjugate addition of the cuprate derived from vinyl bromide **14** and enone (–)-**13** (Scheme 16), the latter prepared during the synthesis of bicycle aldehyde (–)-**5**, would furnish the 2,6-*trans*-disubstituted tetrahydropyranone enolate **110**. Direct capture of this enolate, or that derived from the silyl enol ether with an oxygen source would in turn set the C(10) stereogenicity. Installation of the requisite C(11)–C(12) unsaturation via reduction of the kinetic enol triflate obtained from the C(11) ketone, followed by oxidation state adjustments, would then complete construction of advanced fragment **7**.

Preparation of vinyl bromide **14** entailed Myers alkylation⁷⁷ of the lithium enolate derived from amide (+)-**111** with alkyl iodide **112**, the latter prepared in two-steps and in 93% yield from 1,5-pentanediol (Scheme 33). Amide (+)-**113** was produced both in excellent yield and with high diastereoselectivity (99%, d.r. >20:1). In turn, reduction with $\text{LiAl}(\text{OEt})_3$ generated *in situ*, led directly to aldehyde (–)-**114** in good yield after hydrolysis of the intermediate pseudoephedrine aminal.^{77,78} A Corey–Fuchs homologation/methylation sequence,⁷⁹ followed by hydrozirconation with Schwartz reagent,⁶⁹ and bromination with *N*-bromosuccinimide (NBS) then led to vinyl bromide (–)-**14** as a single stereo- and regioisomer in excellent yield. Overall, vinyl bromide (–)-**14** was prepared in 7 steps (longest linear sequence) and in 55% overall yield from commercially available starting materials.^{12b}

Union of dihydropyranone (–)-**13** with vinyl bromide (–)-**14** entailed addition of the derived cuprate to the Michael acceptor (–)-**13** (Scheme 34); a single diastereomer (–)-**116** resulted with excellent stereocontrol, albeit in modest yield (46%). The proposed Rubottom oxidation however proved problematic, likely due to the ring oxygen. At best a 27% yield of TBS ether (–)-**118** was obtained. Alternate oxidation with either methyl-(trifluoromethyl)dioxirane generated *in situ*,⁸⁰ OsO_4 ,⁸¹ or attempted oxidation of the enolate derived from enol acetate (+)-**117** provided no improvement.

The stereogenicity of the newly generated C(9) and C(10) centers were assigned based on the observed NMR coupling constants of 8.3 Hz and 9.4 Hz (i.e., axial-axial) between H(9) and H(10) in (–)-**118** and (–)-**119**, respectively, indicative of the *trans* relationships.⁸² The absolute stereochemistry of the C(10) center was confirmed via Kakisawa analysis²⁹ of the corresponding Mosher esters derived from alcohol (–)-**119**.

To improve the efficiency of this reaction sequence, we reasoned that the sterically less demanding TES enol ether might be a better oxidation substrate compared to (–)-**116**. We therefore prepared TES enol ether (+)-**120** (Scheme 35), via conjugate addition of the mixed higher-order cuprate [i.e., $\text{R}(2\text{-Th})\text{Cu}(\text{CN})\text{Li}_2$]⁸³ derived from vinyl bromide (–)-**14** and freshly prepared (2-Th)Cu(CN)Li to dihydropyranone (–)-**13**; *in situ* capture of the enolate with triethylsilyl chloride (TESCl) furnished the somewhat hydrolytically unstable TES enol ether (–)-**120** in 77% yield. Purification of (+)-**120** required activity (III) basic alumina to prevent TES hydrolysis.

With (+)-**120** in hand, we installed the requisite C(10) oxygen exploiting the sterically less demanding TES enol ether (Scheme 35). Optimal conditions entailed *m*-CPBA buffered with NaHCO₃ in CH₂Cl₂; (–)-**121** was obtained in 54% yield as a single stereoisomer. Additional screening of the Davis oxaziridines⁸⁴ and magnesium bis(monoperoxyphthalate) (MMPP)⁸⁵ as oxidants proved unrewarding. Utilization of TES enol ether (+)-**120** in place of the TBS ether required the subsequent conversion of TES ether (–)-**121** to the TBS ether (–)-**118**, which was achieved in two-steps (95% yield), that did not require chromatographic purification.

The requisite C(11)–C(12) unsaturation was then installed via kinetic enolate formation (LDA, THF/HMPA), followed in turn by treatment with Comins reagent [*N*-(5-chloro-2-pyridyl)triflimide],⁸⁶ and reduction employing catalytic Pd(PPh₃)₄ with Et₃SiH as the hydride source (Scheme 36).⁸⁷ The observed nOe enhancements between the C(9) methine and the C(14) methylene protons in (–)-**122** confirmed both that the C(9) and C(13) substituents remained *trans* and that the C(13) center had not undergone epimerization via a retro-Michael pathway upon kinetic enolization.

Oxidative removal of the PMB group in (–)-**122**, followed by sequential oxidations employing Dess–Martin⁴³ and Pinnick conditions,⁸⁸ and in turn protection of the resulting carboxylic acid as the *tert*-butyl ester employing *N,N'*-diisopropyl-*O-tert*-butylisourea (**123**),⁸⁹ led to (–)-**124** in 69% yield over the four steps (Scheme 36). Chemoselective removal of the primary TBS group was then achieved with HF•py to furnish the primary alcohol (–)-**125** in 77% yield. Notably, allowing the reaction to proceed to higher conversions led to hydrolysis of the C(10) TBS ether. Dess–Martin oxidation⁸⁸ then completed construction of dihydropyran fragment (–)-**7**. Overall, advanced fragment (–)-**7** was prepared in 19 steps (longest linear sequence) and in 8% overall yield from commercially available starting materials.^{12b}

2.8. Advanced Fragment Union: Unexpected Challenges

Having secured ample quantities of the three major subtargets (–)-**5**, (–)-**6**, and (–)-**7**, we turned to their union via the planned consecutive Julia–Kociński olefinations.⁹⁰ Metallation of sulfone (–)-**6** with LiHMDS, followed by addition of aldehyde (–)-**5** in DMF/HMPA (3:1)⁹¹ provided exclusively the desired *E*-isomer (–)-**126**, as verified by the coupling constant of H(30) (*J* = 15.2 Hz, Entry 1, Table 3). This transformation, although proceeding in low yield (ca. 11–24%), permitted substantial recovery of the coupling partners. Utilizing KHMDS in DME, a set of conditions traditionally employed for *trans* alkene production,⁹¹ led to low *E/Z* selectivity (2:1) with higher conversion (54%, Entry 3). After a variety of different base/solvent combinations were explored (Table 3), best results were achieved with *t*-BuLi in combination with polar aprotic solvents (DMF/HMPA) to furnish (–)-**126** as a single *E* isomer in 39% yield, when run on a 300 mg scale (Entry 5). With several recycles an overall yield of 65% could be achieved.

Turning to the second Julia–Kociński union (Scheme 37), removal of the TBS group in (–)-**126** was achieved with Et₃N•3HF to provide alcohol (–)-**127**, which in turn was subjected to Mitsunobu coupling with phenyltetrazole-thiol (PTSH) followed by molybdenum (VI)-catalyzed oxidation to deliver the PT-sulfone (–)-**128**. The Julia–Kociński union again proved challenging. In this case, the *E/Z* selectivity was reversed, with KHMDS yielding the best *E*-selectivity in DME, with no selectivity observed with LiHMDS in DMF/HMPA. Low conversions were observed in both cases. Validation of the *E*-configuration at C(15)–C(16) also proved less than straightforward, as the H(15) and H(16) vinyl protons shared identical chemical shifts at 5.54 ppm. Recourse was therefore made to the method employed by Höfle and co-workers during their elucidation of (+)-sorangicin A. They assigned the *E*-configuration of the C(15)–C(16) olefin based on the ¹³C

shift of the C(17) carbon at 33.4 ppm, which was in line with theoretical calculations of 33 ppm.⁹² In our case, the chemical shift of the C(17) carbon was 32.7 ppm, supporting the *trans* configuration.

We reasoned the observed low efficiency for both Julia–Kociński unions resides in the nature of the THP-containing sulfones [i.e., (–)-**6** and (–)-**128**]. The combination of difficult initial deprotonations and the presumed resultant intramolecular coordination of the sulfone anions in particular impeded efficient conversion. Reversal of the Julia–Kociński anion and aldehyde coupling partners appeared as a viable option. For the first union however such a reversal would not be without risk, owing to potential β -elimination of the sulfone anion derived from bicycle (–)-**5**. Reversal of coupling partners for the second Julia–Kociński union appeared more feasible (Scheme 38).

Towards this end, conversion of alcohol (–)-**125** to PT-sulfone (+)-**130** was achieved in two steps, and in high overall yield (Scheme 38). More important, use of KHMDS in DME for the Julia–Kociński olefination with aldehyde (–)-**131**, derived from (–)-**127**, provided the coupled product (–)-**129** in high yield (79%) with complete *E*-selectivity. With the second Julia–Kociński olefination efficiently achieved, the three advanced fragments had thus been united. For installation of the *Z,Z,E* trienoate moiety, removal of the silyl group from the secondary TBS ether in (–)-**129** was next readily accomplished, employing solid TBAF·3H₂O, to furnish alcohol (–)-**132**.

2.9. The Sorangicin A Trienoate: A Model Study

Early on Höfle and co-workers demonstrated that the instability of (+)-sorangicin A was a direct result of the resident trienoate system.⁵ In particular, a series of products having undergone isomerization of the trienoate unit were isolated and identified. We of course fully recognized the pending challenge of the sensitive trienoate fragment. Initially we planned to mask the extended unsaturation as a dienyne; model studies thus appeared prudent.

To this end, Stille coupling⁹³ between vinyl iodide (–)-**50** and enyne **8**¹³ proceeded smoothly to furnish dienyne (–)-**133** in 60% yield (Scheme 39). Subsequent semihydrogenation with 5% Pd/CaCO₃, poisoned with Pb, in the presence of quinoline, as expected furnished trienoate **134**, assigned based on ¹H NMR of an unpurified sample. Unfortunately all attempts to remove the excess quinoline, either with NaHSO₄ (1M) or by SiO₂ chromatography, led to rapid isomerization. We therefore abandoned the dienyne tactic and opted to install the C(37)–C(43) fragment with the correct *Z,Z,E* trienoate configuration onto (–)-**132**, with a view to increase convergency.

With this idea in mind, we turned to the use of known stannyl dienoate **135**⁹⁴ bearing the desired *Z,Z*-configuration, which proved to be a stable compound under standard laboratory conditions, due to the electropositive tin stabilizing the electron deficient system as a σ -donor. In a second model study, Stille union between vinyl iodide (–)-**70** and (*Z,Z*)-**135**, employing PdCl₂(PhCN)₂ (5 mol%) proceeded well in terms of yield (96%), albeit a geometric mixture of isomers was obtained, which proved difficult to separate (Entry 1, Table 4). Addition of 1.5 equivalent of Ph₂PO₂NBu₄, an additive generally employed as a tin scavenger to improve coupling efficiency,⁹⁵ did not improve the situation (Entry 2). However, when an excess of Ph₂PO₂NBu₄ (6 equiv) was employed, trienoate (+)-**136** was obtained as a single *Z,Z,E*-isomer in high yield (Entry 3). The requisite *Z,Z,E*-geometry of the extended unsaturation system was assigned based on coupling constants and nOe correlations. Presumably, Ph₂PO₂NBu₄ inhibits *Z/E* isomerization by either arresting formation of detrimental iodide side products, or by accelerating dissociation of the Pd

catalyst after reductive elimination. Of interest, trienoate (+)-**136** proved to be stable for days in CDCl₃, but quickly decomposed in the neat state.

2.10. Elaboration of the Complete Carbon Skeleton of (+)-Sorangicin A

Having succeeded in introducing the trienoate fragment in a simple model, we turned to the construction of the full carbon skeleton (Scheme 40). Pleasingly, the *Z,Z,E*-triene could be introduced in a similar fashion as the model system, albeit an even larger excess of Ph₂PO₂NBu₄ (ca. 12 equiv) was required to furnish (+)-**137** as a single *Z,Z,E*-isomer in 87% yield. Hydrolysis of (+)-**137** was then achieved with LiOH in aqueous THF to provide acid **138** in 70% yield. Although the *Z,Z,E*-configuration was preserved, saponification proceeded quite slowly, with some starting material recovered even after 4 days. To improve the hydrolysis, the methyl ester, dienoate (*Z,Z*)-**139**, was prepared in analogous fashion to (*Z,Z*)-**135** and coupled with vinyl iodide (–)-**132**; again the coupling proved excellent (88%). The hydrolysis now proceeded to completion in 1.5 days to furnish **138**.⁹⁶

2.11. Macrocyclization

With the full carbon skeleton of (+)-sorangicin A assembled, attention shifted to the critical macrocyclization, a task considered nontrivial both due to the hindered C(10) 2°-hydroxyl and the labile trienoacid (Scheme 41). We first selected the conditions of Mukaiyama, as modified by Evans,⁹⁷ given both the convenience of this protocol and the lack of acidic or thermal conditions commonly employed in alternative macrocyclizations that might destroy the sensitive triene. Towards this end, treatment of seco-acid **138** with Mukaiyama reagent **141** and NaHCO₃ in CH₂Cl₂ indeed furnished macrolactone **142**, albeit contaminated with minor amounts of other geometric isomers that proved difficult to remove. Recalling that the Yonemitsu modification of the Yamaguchi conditions,⁹⁸ involving direct introduction of DMAP at room temperature without preformation of the mixed anhydride, had successfully been employed by the Curran group in their total synthesis of (–)-dictyostatin possessing a *Z,E*-dienoacid,⁹⁹ we explored this tactic. Unfortunately, these conditions led to significant isomerization. We reasoned that the formation of geometric isomers might be due to a reversible Michael-type addition of DMAP to the activated trienoacid during the cyclization event. The iodide present in Mukaiyama salt **141** held a similar risk. Another risk associated with activator **141** was halogen exchange leading to **143**, a reagent known to be inert toward carboxylic acid activation.¹⁰⁰

To address these issues, the modified Mukaiyama reagent **144** was adopted, which possesses a non-nucleophilic counterion, tetrafluoroborate, envisioned to mitigate both isomerization and inactivation pathways.¹⁰¹ Pleasingly, macrolide **142** was obtained in excellent yield (80%), with minimum isomerization (<10%) under dilute conditions (*c*≤1×10^{–3} M), employing **144** (Scheme 42). Moreover, the *Z,Z,E*-triene configuration was retained, as confirmed from the observed NMR coupling constants (Scheme 42). In this case, the larger 1-ethyl group in **144**, may also contribute to the success, by suppressing decomposition of the pyridinium salt, a result of attack on the 1-alkyl group, while at the same time not being too sterically encumbered to hinder cyclization upon acid activation.

2.12. Global Deprotection: A Challenging Transformation

All that remained to complete the total synthesis of (+)-sorangicin A (**1**) was to define suitable conditions to remove the three acid labile protecting groups: the *t*-butyl ester, the acetonide, and the MOM ether group, while maintaining the delicate macrocycle. This proved to be a daunting task, due to the proclivity of the macrolide to undergo isomerization of the (*Z,Z,E*)-trienoate. As noted in the introduction, Höfle and coworkers demonstrated that natural (+)-sorangicin A (**1**) could be protected efficiently as acetonide **145** with TFA in acetone (ca. 98%), and that deprotection could be achieved in 70% yield employing TFA in

aqueous THF at 85 °C (Scheme 43).¹⁴ Indeed, exploiting this protocol they prepared an extensive library of sorangicin analogues. The efficiency of deprotection however was highly substrate-dependent, ranging from 20% to 50%.

With this in mind, treatment of the fully protected macrolide **142** with TFA in aqueous THF, first at room temperature, led to acetonide removal, a process that was accelerated by silica gel (Scheme 44). Additional heating at 85 °C did not lead to further deprotection; only decomposition occurred.

Encouraged by our ability to remove the acetonide, we initiated a series of deprotection studies on the more readily available, advanced fragments (+)-**108** and (-)-**125** to preserve the valuable macrolide **142**. These efforts demonstrated that aqueous TFA/THF conditions would remove the acetonide in (+)-**108** at 45 °C, and when the temperature was raised to 85 °C the MOM group (Scheme 45A). Liberation of the acid from *t*-butyl ester (-)-**125** (Scheme 45B) however could only be achieved in 42% yield at 85 °C, indicating that a more effective protocol had to be devised to hydrolyze the *t*-butyl ester. Anhydrous TFA in CH₂Cl₂ was not an option, as decomposition of the delicate trienoate linkage proved competitive. Turning to Lewis acids, *B*-bromocatecholborane¹⁰² removed both the MOM and acetonide groups in (+)-**108**, but removal of the *t*-butyl group of the ester remained sluggish (Scheme 45C and D).

Subsequent screening revealed that treatment of (-)-**125** with TMSOTf in 2,6-lutidine liberated the acid with good overall efficiency, after an acidic workup (1M KHSO₄) (88%, Scheme 46). These conditions also cleanly removed the MOM group in (+)-**108**. With these observations in hand, we attempted to remove both the MOM and *t*-butyl groups simultaneously, employing late stage intermediate **142**. Only decomposition resulted!

We reasoned that TMSOTf was sufficiently powerful to liberate the acid from the *t*-butyl ester, but too reactive to maintain the delicate trienoate. In the end, we discovered that TBSOTf, a bulkier reagent, buffered with 2,6-lutidine, fulfilled both the requirements: selective removal of the *t*-butyl group without compromising the (*Z,Z,E*)-trienoate linkage to furnish the now TBS protected ester **153**, after an acid workup (0.2 N HCl) (Scheme 47). Notably, the MOM and acetonide protecting groups in **142** were not affected by these conditions. Treatment of TBS ester **153** with *B*-bromocatecholborane at low temperature then furnished the fully deprotected macrolide **154**.

2.13. The Structure of (+)-Sorangicin A

With the first synthetic sample of the fully deprotected macrolide **154** in hand, careful comparison of the TLC of an authentic sample of (+)-sorangicin A (**1**), kindly provided by Höfle, with a sample of the synthetic macrolide was not promising, although high-resolution mass spectroscopy confirmed the correct molecular formula. The 500 MHz ¹H NMR spectrum of **154**, albeit not pure, clearly indicated that the trienoate remained intact during the two-step deprotection process.

Before committing additional, highly valuable advanced materials to provide access to pure **154** for detailed NMR analysis, we compared the 500 MHz ¹H NMR spectrum of natural (+)-sorangicin A in CD₃OD with that of the synthetic protected pure macrolide **142**, having assigned the majority of the resonances in the latter via extensive 2D NMR experiments (Figure 6). This analysis revealed that: (a) the trienoate regions matched closely; (b) the C(21)–C(23) segments did not resemble each other, an understandable observation given the local conformational effects arising from the acetonide in **142**; and (c) significant differences in chemical shifts and line shapes were observed for three vinyl protons: H(7), H(11) and H(12). We thereby suspected that the structure of the dihydropyran ring, and in

particular the C(10) stereochemical center in **142** was not consistent with (+)-sorangicin A (**1**).

Given that single-crystal X-ray structure **155**⁴ (Figure 7) had been employed by Höfle and coworkers to confirm their initial structure assignment of (+)-sorangicin A (**1**), an error involving the misassignment of backbone connectivity or relative stereochemistry was eliminated. Review of the original 1989 publication⁴ revealed that (+)-sorangicin A was depicted as **156** with *S*-C(10) configuration (Figure 7). However, in a later publication (1993),⁶ a publication that we had relied upon, Höfle and co-workers depicted (+)-sorangicin A as structure **3** with the C(10) *R* configuration. Clearly the *R* configuration at C(10) in synthetic **142** led to the discrepancies of the H(7), H(11) and H(12) resonances in our synthetic material.

2.14. In-House X-Ray Analysis of (+)-Sorangicin A (**1**)

Before taking final action to complete the total synthesis of (+)-sorangicin A (**1**), we conducted an X-ray analysis of natural (+)-sorangicin A, kindly provided by Dr. Rolf Jansen. By collecting the X-ray intensity data at low temperature, 143 K, compared to the Höfle analysis at 293 K, we not only confirmed the *S* configuration at C(10), but also provided new information on the dynamic disorder identified by the Höfle team.⁴ In particular, the C(16)–C(17)–C(18) moiety was disordered by rotation of approximately 30° about the C(14)–C(15) and C(19)–C(20) bonds, which upon refinement of two contributing disorder fragments [C(16), C(17), C(18), and C(16'), C(17'), C(18')] with 50% occupancies, gave rise to high resolution structures that confirmed the single bond nature of the C(17)–C(18) moiety, a matter of early concern in the initial structure analysis (Figure 8). The reader will recall that the high flexibility of the C(14)–C(20) region had been correlated with the superior adaptive ability of (+) sorangicin A (**1**) towards microbial mutation, leading to an advantageous cross-resistant profile over rifampicin (**2**), a discovery with clear implications vis-à-vis future drug design and development against fast evolving microbes.³

2.15. Inversion of the C(10) Stereogenicity: Access Advanced Intermediate **161**

We began with global desilylation of (–)-**124**, followed by selective silylation of the primary hydroxyl group to furnish allylic alcohol (–)-**158** in excellent yield (Scheme 48). Attempts to invert the C(10) center employing a variety of Mitsunobu conditions failed due to intervention of an S_N2' pathway, presumably due to the bulky nature of the C(1)–C(8) side chain. Recourse to a Ley oxidation¹⁰³/Luche reduction¹⁰⁴ sequence however quickly delivered the desired allylic alcohol (+)-**159** as a single diastereomer. Pleasingly, the line shape of H(9) in the ¹H

NMR of (+)-**159** changed from a doublet (*J* = 7.1 Hz) as in (–)-**158** to a singlet after inversion, closely resembling that of the natural product. Protecting group manipulations followed by introduction of the sulfone unit employing the conditions developed earlier (Scheme 38) completed construction of (+)-**161**. The eight step sequence proceeded in 46% yield.

2.16. Completion of the First Total Synthesis of (+)-Sorangicin A (**1**)

With the stereogenicity at C(10) now secure, Julia–Kociński union between aldehyde (–)-**131** and sulfone (+)-**161** proceeded smoothly to furnish vinyl iodide (+)-**162** after desilylation (Scheme 49). Additional (+)-**162** was also available via an oxidation/reduction sequence employing advanced intermediate (–)-**132**. Conversion of (+)-**162** to (+)-sorangicin A (**1**) now proved straight forward. Importantly the critical Mukaiyama macrolactonization was highly efficient (88%). Finally, somewhat more effective conditions to remove the MOM, acetamide, and TBS protecting group, employing 4N HCl in THF, led

to synthetic (+)-sorangicin A (**1**). Interestingly, (+)-sorangicin A proved stable to strong aqueous protic acid in the absence of oxygen over 24 h. The overall yield for the five steps was 45%. Synthetic (+)-sorangicin A (**1**) proved to be indistinguishable from an authentic sample of **1** by NMR, mass spectrometric, and chromatographic comparisons (three solvent systems).^{12d} Moreover, the chiroptic properties { $[\alpha]_D^{19}$: +56 (c 0.06, MeOH); lit.⁴ $[\alpha]_D^{22}$: +60.9 (c 0.7, MeOH) } confirmed that the absolute configuration of (+)-sorangicin A is as depicted in **1**, consistent with the X-ray analysis achieved by Höfle and co-workers.⁴

3. Conclusion

The first and to date only total synthesis of (+)-sorangicin A (**1**) has been achieved. The longest linear sequence was 30 steps that proceeded in 3.2% overall yield. The enantioselective route features high convergency, as well as a number of key features and/or tactics, including: a first- and second-generation synthesis of the dioxabicyclo[3.2.1]octane core, effective constructions of the advanced di- and tetrahydropyran ring systems, consecutive Julia–Kociński olefinations to unite three advanced fragments with high *E*-stereoselectivity, a modified Stille union to introduce the sensitive *Z,Z,E* triene functionality, a highly efficient Mukaiyama macrolactonization, and carefully defined Lewis and protic acid-promoted deprotection protocols to achieve global deprotection in the final stage of the synthetic venture.

Supplementary Material

Refer to Web version on PubMed Central for supplementary material.

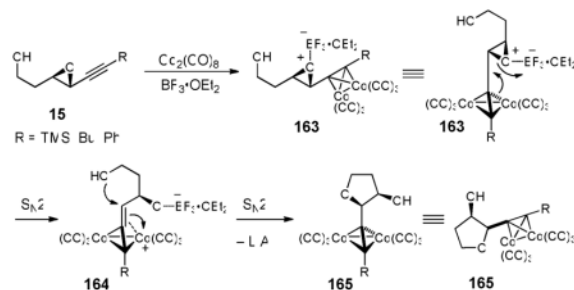
Acknowledgments

This article is dedicated to Professor Gilbert Stork (Columbia University), outstanding scientist, scholar and friend, on the occasion of his 90th birthday. Over nearly 70 years, Professor Stork and his group have transformed the field of Synthetic Organic Chemistry that now make possible total syntheses such as (+)-sorangicin A. Happy Birthday Gilbert!!! Support was provided by the National Institutes of Health (National Institute of General Medical Sciences) through Grant GM-29028. We also thank Drs. George Furst, Rakesh Kohli and Patrick Carroll (University of Pennsylvania) for assistance in obtaining NMR spectra, high resolution mass spectra, and X-ray crystallographic data, respectively. We also thank Dr. Rolf Jansen (Helmholtz Center for Infection Research, Braunschweig, Germany) for an authentic sample of (+)-sorangicin A.

References and notes

1. Jansen R, Wray V, Irschik H, Reichenbach H, Höfle G. *Tetrahedron Lett.* 1985; 26:6031.
2. Irschik H, Jansen R, Gerth K, Höfle G, Reichenbach H. *J Antibiot.* 1987; 40:7. [PubMed: 3104268]
3. Campbell EA, Pavlova O, Zenkin N, Leon F, Irschik H, Jansen R, Severinov K, Darst SA. *The EMBO Journal.* 2005; 24:674. and references cited therein. [PubMed: 15692574]
4. Jansen R, Irschik H, Reichenbach H, Schomburg D, Wray V, Höfle G. *Liebigs Ann Chem.* 1989; 111
5. Jansen R, Irschik H, Reichenbach H, Wray V, Höfle G. *Liebigs Ann Chem.* 1989; 213
6. Schummer D, Irschik H, Höfle G. *Liebigs Ann Chem.* 1993; 293
7. Danek, SC. PhD Thesis. Morken Group, University of North Carolina; Chapel Hill: 2003.
8. Schinzer D, Schulz C, Krug O. *Synlett.* 2004; 15:2689.
9. Park SH, Lee HW. *Bull Korean Chem Soc.* 2008; 29:1661.
10. (a) Srihari P, Kumaraswamy B, Yadav JS. *Tetrahedron.* 2009; 65:6304. (b) Mohapatra DK, Das PP, Pattanayak MR, Yadav JS. *Chem Eur J.* 2010; 16:2072. [PubMed: 20099288]
11. (a) Crimmins MT, Haley MW. *Org Lett.* 2006; 8:4223. [PubMed: 16956192] (b) Crimmins MT, Haley MW, O'Bryan EA. *Org Lett ASAP.* 10.1021/ol201920j

12. (a) Smith AB III, Fox RJ. *Org Lett.* 2004; 6:1477. [PubMed: 15101771] (b) Smith AB III, Fox RJ, Vanecko JA. *Org Lett.* 2005; 7:3099. [PubMed: 15987215] (c) Smith AB III, Dong S. *Org Lett.* 2009; 11:1099. [PubMed: 19182995] (d) Smith AB III, Dong S, Brenneman JB, Fox RJ. *J Am Chem Soc.* 2009; 131:12109. [PubMed: 19663510]
13. Rossi R, Bellina F, Catanese A, Mannina L, Valensin D. *Tetrahedron.* 2000; 56:479.
14. Jansen R, Schummer D, Irschik H, Höfle G. *Liebigs Ann Chem.* 1990; 975
15. (a) Ferrier RJ, Middleton S. *Chem Rev.* 1993; 93:2779. (b) Petasis NA, Lu SP. *Tetrahedron Lett.* 1996; 37:141. (c) Smith AB III, Fox RJ, Razler TM. *Acc Chem Res.* 2008; 41:675. [PubMed: 18489082] For examples exploiting the Petasis-Ferrier union/rearrangement tactic in natural product synthesis, see: (d) Smith AB III, Minbiolo KP, Verhoest PR, Schelhaas M. *J Am Chem Soc.* 2001; 123:10942. [PubMed: 11686698] (e) Smith AB III, Verhoest PR, Minbiolo KP, Lim JJ. *Org Lett.* 1999; 1:909. [PubMed: 10823221] (f) Smith AB III, Minbiolo KP, Verhoest PR, Beauchamp TJ. *Org Lett.* 1999; 1:913. [PubMed: 10823222] (g) Smith AB III, Sfougatakis C, Gotchev DB, Shirakami S, Bauer D, Zhu W, Doughty VA. *Org Lett.* 2004; 6:3637. [PubMed: 15387567] (h) Smith AB III, Safonov IG, Corbett RM. *J Am Chem Soc.* 2002; 124:11102. [PubMed: 12224958] (i) Smith AB III, Safonov IG, Corbett RM. *J Am Chem Soc.* 2001; 123:12426. [PubMed: 11734051] For more recent modifications, see: (j) O'Neil KE, Kingree SV, Minbiolo KPC. *Org Lett.* 2005; 7:515. [PubMed: 15673278]
16. Redlich H, Bruns W, Francke W, Schuring V, Payne TL, Vite JP. *Tetrahedron.* 1987; 2029
17. Keck GE, Li X-Y, Krishnamurthy D. *J Org Chem.* 1995; 60:5998.
18. Mukai C, Sugimoto Y-i, Ikeda Y, Hanaoka M. *J Chem Soc Chem Commun.* 1994; 1161
19. Nicholas KM. *Acc Chem Res.* 1987; 20:207–214.
20. Upon generation of the activated complex **163**, an anchimeric assisted S_N2 epoxide ring-opening, via $\text{Co}_2(\text{CO})_6$ -alkyne complex, initially furnishes intermediate **164**. See (a) Schreiber SL, Sammakia T, Crowe WE. *J Am Chem Soc.* 1986; 108:3128. (b) Schreiber SL, Klimas MT, Sammakia T. *J Am Chem Soc.* 1987; 109:5749. Intramolecular S_N2 capture of cation **164** by the hydroxy group, from the same face as the epoxide, then leads to the $\text{Co}_2(\text{CO})_6$ -alkyne complex (**165**) with overall retention of stereochemistry. See: Mukai C, Sugimoto Y-i, Ikeda Y, Hanaoka M. *Tetrahedron.* 1998; 54:823.



21. Seng F, Negishi E-I. *Org Lett.* 2001; 3:719. [PubMed: 11259045] For related compounds and applications, see (b) Negishi E-I, Alimardanov A, Xu C. *Org Lett.* 2000; 2:65. [PubMed: 10814247] (c) Negishi E-I, Hata M, Xu C. *J Am Chem Soc.* 2003; 125:13636. [PubMed: 14599182]
22. For the preparation of the enantiomer of (+)-**28**, see Zheng W, DeMattei JA, Wu J-P, Duan JJ-W, Cook LR, Oinuma H, Kishi Y. *J Am Chem Soc.* 1996; 118:7946.

23. (a) England P, Chun KH, Moran EJ, Armstrong RW. *Tetrahedron Lett.* 1990; 31:2669. (b) Ishihara J, Mikakawa J, Tsujimoto T, Murai A. *Synlett.* 1997:1417. (c) Chênevert R, Dasser M. *J Org Chem.* 2000; 65:4529. [PubMed: 10959854] (d) Keck GE, Wager CA, Wager TT, Savin KA, Covell JA, McLaws MD, Krishnamurthy D, Cee VJ. *Angew Chem Int Ed.* 2001; 40:231. (e) Piggott MJ, Wege D. *Aust J Chem.* 2003; 56:691. (f) Marshall JA, Schaaf GM. *J Org Chem.* 2003; 68:7428. [PubMed: 12968896]
24. Bailey S, Harnden MR, Jarvest RL, Parkin A, Boyd MR. *J Med Chem.* 1991; 34:57. [PubMed: 1846922]
25. Veysoglu T, Mitscher LA, Swayze JK. *Synthesis.* 1980; 807
26. Kjell DP, Slattery BJ, Semo MJ. *J Org Chem.* 1999; 64:5722. [PubMed: 11674650]
27. (a) Brown HC, Bhat KS. *J Am Chem Soc.* 1986; 108:293. (b) Brown HC, Bhat KS. *J Am Chem Soc.* 1986; 108:5919. [PubMed: 22175350]
28. (a) Crispino GA, Jeong K-S, Kolb HC, Wang Z-M, Xu D, Sharpless KB. *J Org Chem.* 1993; 58:3785. and references cited therein. (b) Kolb HC, VanNieuwenhze MS, Sharpless KB. *Chem Rev.* 1994; 94:2483.
29. Ohtani I, Kusumi T, Kashman Y, Kakisawa H. *J Am Chem Soc.* 1991; 113:4092.
30. (a) Rychnovsky SD, Skalitzky DJ. *Tetrahedron Lett.* 1990; 31:945. (b) Evans DA, Rieger DL, Gage JR. *Tetrahedron Lett.* 1990; 31:7099.
31. Hicks DR, Fraser-Reid B. *Synthesis.* 1974; 203
32. Dounay AB, Florence GJ, Saito A, Forsyth CJ. *Tetrahedron.* 2002; 58:1865.
33. Whereas vinyl bromide **24** has been reported to be a competent component in cross-coupling reactions, anions derived from **24** have not been described.
34. Although commercially available, 1,4-bis(trimethylsilyl)-1,3-butadiyne was prepared on large-scale according to (a) Jones GE, Kendrick DA, Holmes AB. *Organic Syntheses, Coll.* 865:63. 52. For the initial preparation of 1,4-bis(trimethylsilyl)-1,3-butadiyne, see (b) Walton DRM, Waugh F. *J Organometallic Chem.* 1972; 37:45. See Supporting Information for details.
35. (a) Bohlmann F, Enkelmann R, Plettner W. *Chem Ber.* 1964; 97:2118. (b) Doolittle RE. *Synthesis.* 1984:730.
36. (a) While Holmes and co-workers reported the generation of lithium trimethylsilylbutadiyne from 1,4-bis(trimethylsilyl)-1,3-butadiyne (**33**), followed by reaction with a wide range of alkyl halides and carbonyl compounds, examples of epoxide ring-opening by lithium trimethylsilylbutadiyne have not been recorded (b) Holmes AB, Jennings-Whie CLD, Schulthess AH. *J Chem Soc Chem Comm.* 1979:840. (c) Holmes AB, Jones GE. *Tetrahedron Lett.* 1980; 21:3111.
37. Crousse B, Alami M, Linstrumelle G. *Synlett.* 1997; 992
38. Studies on the LiAlH_4 reduction of propargylic alcohols and 4-substituted-3-butyne-1-ols suggest that the mechanism may be more complicated. See (a) Molloy BB, Hauser KL. *J Chem Soc Chem Commun.* 1968:1017. (b) Borden WT. *J Am Chem Soc.* 1970; 92:4898. (c) Grant B, Djerassi C. *J Org Chem.* 1974; 39:968. (d) Kang MJ, Jang J-S, Lee S-G. *Tetrahedron Lett.* 1995; 36:8829.
39. (a) Wang Z-X, Tu Y, Frohn M, Zhang J-R, Shi Y. *J Am Chem Soc.* 1997; 119:11224. (b) Wang Z-X, Shi Y. *J Org Chem.* 1998; 63:3099. For epoxidation of enyne systems, see (c) Wang Z-X, Cao G-A, Shi Y. *J Org Chem.* 1999; 64:7646. For a recent review, see (d) Shi Y. *Acc Chem Res.* 2004; 37:488. [PubMed: 15311947]
40. The reaction was also executed in the extremely polar $\text{LiClO}_4 \cdot \text{OEt}_2$ solvent system developed by the Dailey and Grieco groups, with the idea of increasing carbocationic character in the ring-opening transition state. Although the reaction rate was enhanced dramatically, the ratio of (-)-**21** to (-)-**45** remained nearly 1:1. See: (a) Grieco PA, Nunes JJ, Gaul MD. *J Am Chem Soc.* 1990; 112:4595. (b) Grieco PA, Kisakürek V. *Organic Chemistry in Lithium Perchlorate/Diethyl Ether. Organic Chemistry: Its Language and Its State of the Art.* VCHBasel1993:133. (c) Forman MA, Dailey WP. *J Am Chem Soc.* 1991; 113:2761.
41. It is important to note that in the conversion of (+)-**49** to (-)-**46**, degassing of all solvents (i.e., CH_2Cl_2 and MeOH) was imperative to achieve high yields reproducibly, indicating the high air sensitivity of the reaction.
42. Burchat AF, Chong JM, Nielson N. *J Organometallic Chem.* 1997; 542:281.
43. Dess DB, Martin JC. *J Org Chem.* 1983; 48:4155.

44. For an example of an alkyne possessing both α - and β -ether substituents proceeding with excellent regioselectivity to furnish the β -isomer, see Mukai C, Miyakoshi N, Hanaoka M. *J Org Chem.* 2001; 66:5875. [PubMed: 11511265]
45. Although reproducible, the synthetic yield and enantioselectivity for (–)-**13** was highly dependent on the degree of molecular sieve activation based on Keck's protocol as in ref. 17.
46. Danishefsky S, Kitahara T. *J Am Chem Soc.* 1974; 96:7807.
47. Cardani S, Toma CD, Gennari C, Scolastico C. *Tetrahedron.* 1992; 48:5557.
48. (a) Dossetter AG, Jamison TF, Jacobsen EN. *Angew Chem Int Ed.* 1999; 38:2398.(b) Gademann K, Chavez DE, Jacobsen EN. *Angew Chem Int Ed.* 2002; 41:3059.
49. Paterson I, Steven A, Luckhurst CA. *Org Biomol Chem.* 2004; 2:3026. [PubMed: 15480468]
50. (a) Alexakis A, Vastra J, Mangeney P. *Tetrahedron Lett.* 1997; 38:7745.(b) Agapiou K, Cauble DF, Krische MJ. *J Am Chem Soc.* 2004; 126:4528. [PubMed: 15070365]
51. Hutchinson DK, Fuchs PL. *J Am Chem Soc.* 1987; 109:4930.
52. Suzuki M, Morita Y, Koyano H, Koga M, Noyori R. *Tetrahedron.* 1990; 46:4809.
53. Fürstner A, Grell K, Mathes C, Lehmann CW. *J Am Chem Soc.* 2000; 122:11799.
54. Joly GD, Jacobsen EN. *Org Lett.* 2002; 4:1795. [PubMed: 12000301]
55. Aldehyde (–)-**58**, although commercially available, was prepared in two steps from L-gulonic acid γ -lactone; see Hubschwerlen C, Specklin JL, Higelin J. *Organic Syntheses.* 1995; 72:1.
56. That is, during the enolate alkylation, which is a very slow process, the Zn-methyl group of **60** is sufficiently basic, in the presence of excess HMPA, to deprotonate (+)-**61**; the resulting secondary kinetic enolate then reacts with MeI to yield side product (+)-**62**, see: Rathgeb X, March S, Alexakis A. *J Org Chem.* 2006; 71:5737. [PubMed: 16839156] Lowering the alkylation temperature from –40 °C to –60 °C led to a slower reaction and in turn an increase of (+)-**62** (38%). Higher temperatures (ca. –20 °C) however had a beneficial effect on the yield of (+)-**61**, but did not rectify the problem completely. Application of the more active alkylation reagent MeOTf proved no better.
57. Kojima N, Maezaki N, Tominaga H, Asai M, Yanai M, Tanaka T. *Chem Eur J.* 2003; 9:4980. [PubMed: 14562316]
58. Parikh J, Doering W. *J Am Chem Soc.* 1967; 89:5505.
59. Takai K, Nitta K, Utimoto K. *J Am Chem Soc.* 1986; 108:7408.
60. Kende AS, DeVita RJ. *Tetrahedron Lett.* 1990; 31:307.
61. Evans DA, Black WC. *J Am Chem Soc.* 1993; 115:4497.
62. Seebach D, Imwinkelried R, Stucky G. *Helv Chim Acta.* 1987; 70:448.
63. Petasis NA, Bzowej EI. *J Am Chem Soc.* 1990; 112:6392.
64. Although dioxanone formation and methylenation proceeded smoothly, attempts to perform the rearrangement with an acetonide at C(21,22) led to decomposition.
65. Cossey KN, Funk RL. *J Am Chem Soc.* 2004; 126:12216. [PubMed: 15453725]
66. This highly selective aldol strategy has been successfully applied by the Crimmins group in the synthesis of (+)-spongistatin 1, in which the α and β oxygen substituents of a methyl ketone acted in synergy to deliver a single diastereomeric aldol adduct, see: Crimmins MT, Katz JD, McAtee LC, Tabet EA, Kirincich SJ. *Org Lett.* 2001; 3:949. [PubMed: 11263923]
67. Marshall JA, Seletsky JA, Boris M, Luke GP. *J Org Chem.* 1994; 59:3413.
68. (a) Miwa K, Aoyama T, Shioiri T. *Synlett.* 1994:107.(b) Myers AG, Goldberg SD. *Angew Chem, Int Ed.* 2000; 29:2732.
69. Hart DH, Blackburn TF, Schwartz J. *J Am Chem Soc.* 1975; 97:679.
70. Miyaura N, Suzuki A. *Chem Rev.* 1995; 95:2457.
71. Alkyl boronate **76** was prepared from 1,3-propanediol; see Supporting Information
72. Shekhani MS, Khan KM, Mahwood K, Shah PM, Malik S. *Tetrahedron Lett.* 1990; 31:1669.
73. Rauhala V, Nevalainen M, Koskinen AMP. *Tetrahedron.* 2004; 60:9199.
74. Paterson I, Coster MJ, Chen DY-K, Aceña JL, Bach J, Keown LE, Trieselmann T. *Org Biomol Chem.* 2005; 3:2420. [PubMed: 15976859]

75. One possible explanation for the observed decrease in C(25) OH elimination upon changing the reaction solvent from CH₂Cl₂ to CH₃CN is that the Lewis basic CH₃CN attenuated the Lewis acidity of the BF₃•OEt₂.
76. Schultz HS, Freyermuth HB, Buc SR. *J Org Chem.* 1963; 28:1140.
77. Myers AG, Yang BH, Chen H, McKinstry L, Kopecky DJ, Gleason JL. *J Am Chem Soc.* 1997; 119:6496.
78. The stereochemical outcome for the Myers alkylation and reduction protocol was confirmed via reduction of aldehyde (–)-**114** to the corresponding alcohol, removal of the PMB ether and conversion to the known bis-Mosher esters, see Kubota T, Tsuda M, Kobayashi J. *J Org Chem.* 2002; 67:1651. and references cited therein. [PubMed: 11871898]
79. Corey EJ, Fuchs PL. *Tetrahedron Lett.* 1972; 36:3769.
80. (a) Yang DY, Wong M-K, Yip Y-C. *J Org Chem.* 1995; 60:3887.(b) Thompson CF, Jamison TF, Jacobsen EN. *J Am Chem Soc.* 2001; 123:9974. [PubMed: 11592876]
81. (a) McCormick JP, Tomasik W, Johnson MW. *Tetrahedron Lett.* 1981; 22:607.(b) Boeckman RK Jr, Starrett JE Jr, Nickell DG, Sum P-E. *J Am Chem Soc.* 1986; 108:5549.
82. This assignment is based on the precedent that 236-trisubstituted tetrahydropyranones approximate chair conformations see: Goodwin TE, Crowder CM, White RB, Swanson JS. *J Org Chem.* 1983; 48:376.
83. (a) Lipshutz BH, Kozlowski JA, Parker DA, Nguyen SL, McCarthy KE. *J Organometallic Chem.* 1985; 285:437.(b) Lipshutz BH, Koerner M, Parker DA. *Tetrahedron Lett.* 1987; 28:945.
84. (a) Davis FA, Sheppard AC. *J Org Chem.* 1987; 52:955.(b) Davis FA, Lal SG. *J Org Chem.* 1988; 53:5004.(c) Davis FA, Chattopadhyay S, Towson JC, Lal S, Reddy T. *J Org Chem.* 1988; 53:2087.and (d) Vishwakarma LC, Stringer OD, Davis FA. *Organic Syntheses, Coll.* 866:546. 203.
85. Brougham P, Cooper MS, Cummerson DA, Heaney H, Thompson N. *Synthesis.* 1987; 1015
86. (a) Comins DL, Dehghani A. *Tetrahedron Lett.* 1992; 33:6299.(b) Comins DL, Dehghani A, Foti CJ, Joseph SP. *Organic Syntheses, Coll.* 974:165. 77.
87. Scott WJ, Stille JK. *J Am Chem Soc.* 1986; 108:3033.
88. Bal BS, Childers WE Jr, Pinnick HW. *Tetrahedron.* 1981; 37:2091.
89. For a review on isourea reagent see Mathias LJ. *Synthesis.* 1979; 561
90. Blakemore PR, Cole WJ, Kocienski PJ, Morley A. *Synlett.* 1998; 26
91. Liu P, Jacobsen EN. *J Am Chem Soc.* 2001; 123:10772. [PubMed: 11674024]
92. In the structural elucidation paper of sorangicin A by Höfle et al., ref. 1, based on assumption of additivity of effects and the known carbon chemical shifts of hexa-1,5-diene, *E*- and *Z*-hex-3-ene and but-1-ene, the authors calculated the carbon chemical shifts of C(17) in the *E*- and *Z*-configuration to be *ca.* 33 and 27 ppm, respectively.
93. (a) Milstein D, Stille JK. *J Am Chem Soc.* 1978; 100:3636.(b) Stille JK. *Angew Chem Int Ed.* 1986; 25:508.
94. Franci X, Martina SLX, McGrady JE, Webb MR, Donald C, Taylor RJK. *Tetrahedron Lett.* 2003; 44:7735.
95. Srogl J, Allred GD, Liebeskind LS. *J Am Chem Soc.* 1997; 119:12376.
96. Acid **138** proved to be extremely unstable, and therefore was employed in the next step without full characterization.
97. (a) Mukaiyama T, Usui M, Saigo K. *Chem Lett.* 1976:49.(b) Evans DA, Starr JT. *J Am Chem Soc.* 2003; 125:13531. [PubMed: 14583050]
98. (a) Inanaga J, Hirata K, Saeki H, Katsuki T, Yamaguchi M. *Bull Chem Soc Jpn.* 1979; 52:1989.(b) Hikota M, Sakurai Y, Horita K, Yonemitsu O. *Tetrahedron Lett.* 1990; 31:6367.
99. Shin Y, Fournier J-H, Brückner A, Madiraju C, Balachandran R, Raccor BS, Edler MC, Hamel E, Sikorski RP, Vogt A, Day BW, Curran DP. *Tetrahedron.* 2007; 63:8537. [PubMed: 18728696]
100. (a) Oh SH, Cortez GS, Romo D. *J Org Chem.* 2005; 70:2835. [PubMed: 15787582] (b) Bradlow HL, Vanderwerf CA. *J Org Chem.* 1951; 16:1143.
101. (a) Xu JC, Li P. *Tetrahedron.* 2000; 56:8119.For advantages of using modified Mukaiyama reagents, see: (b) Folmer JJ, Acero C, Thai DL, Rapoport H. *J Org Chem.* 1998; 63:8170.

102. Boeckman RK Jr, Potenza JC. *Tetrahedron Lett.* 1985; 26:1411.
103. Ley SV, Norman J, Griffith WP, Marsden SP. *Synthesis.* 1994; 639
104. Luche JL. *J Am Chem Soc.* 1978; 100:2226.

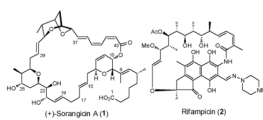


Fig 1.
Structures of (+)-Sorangicin A (1) and Rifampicin (2)

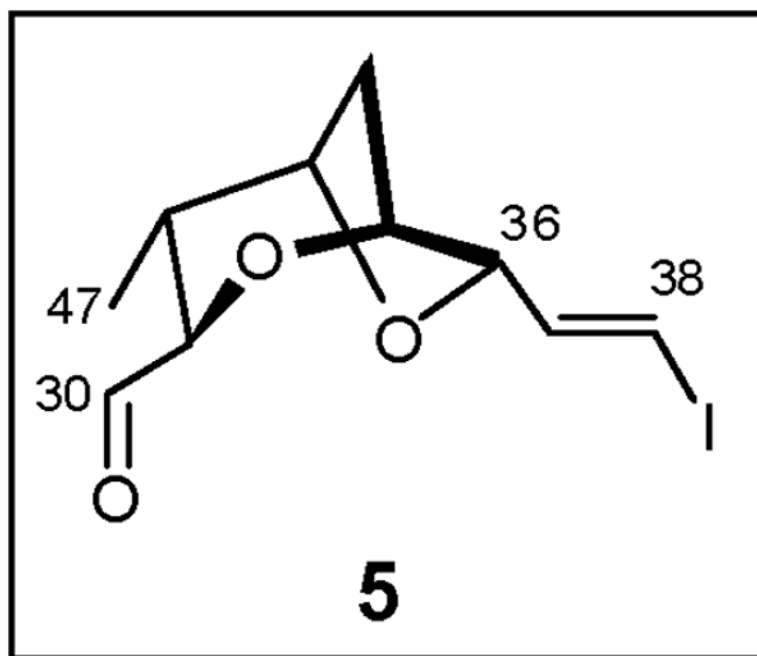


Fig 2.
Structure of Bicyclic Fragment 5

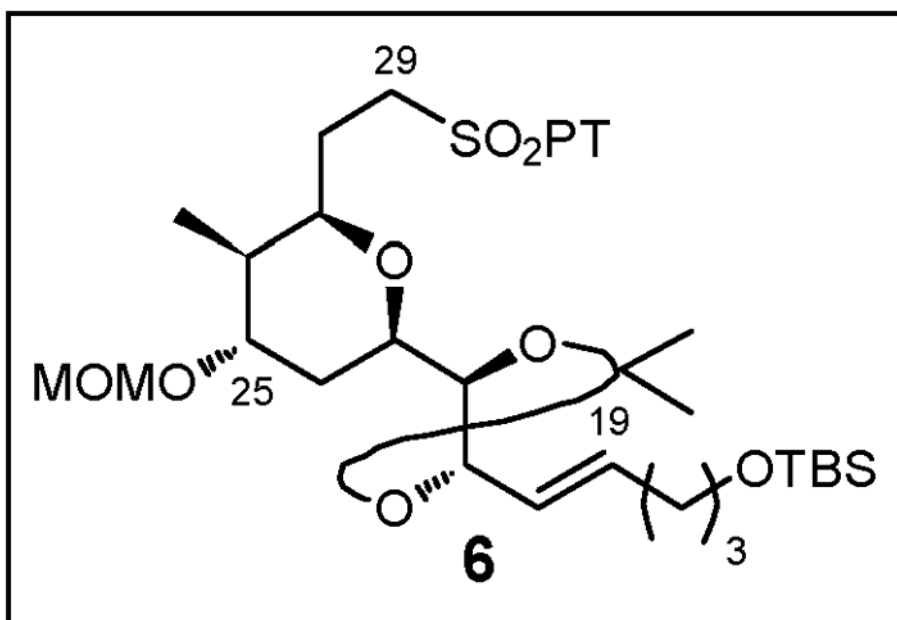


Fig 3.
Structure of THP Fragment 6

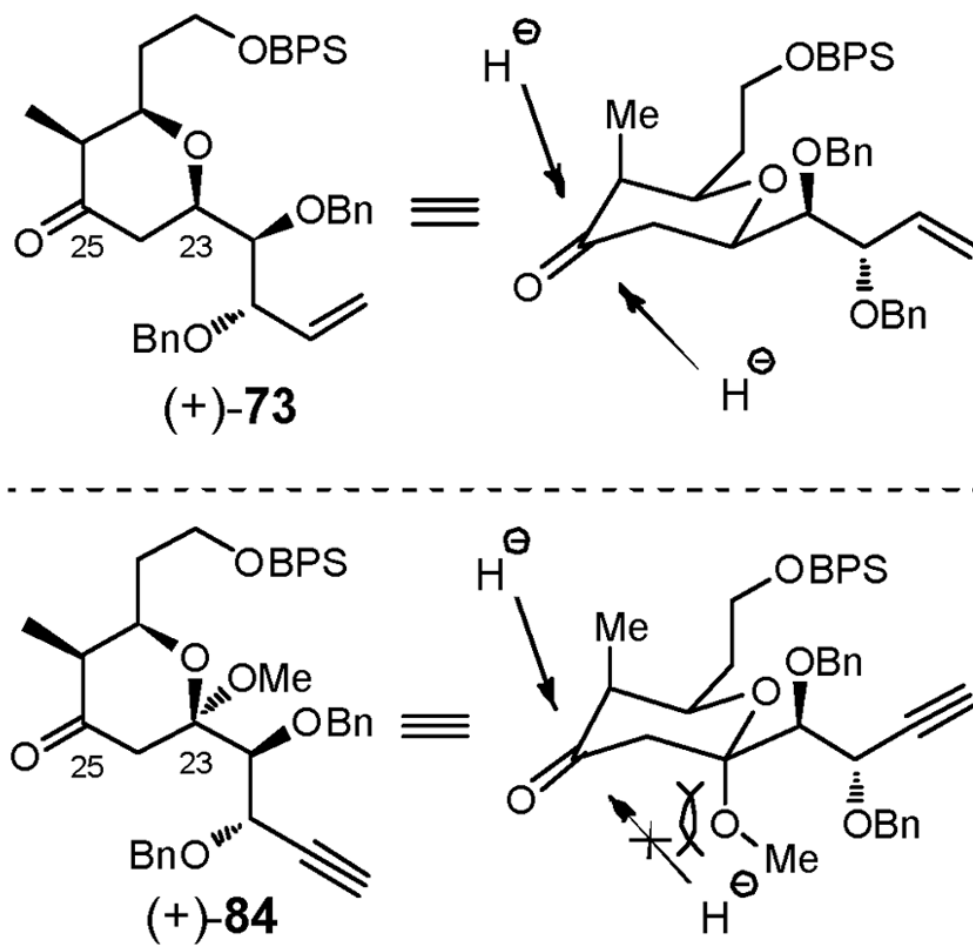


Fig 4.
Rationale for observed stereoselectivity in the reduction of (+)-73 and (+)-84

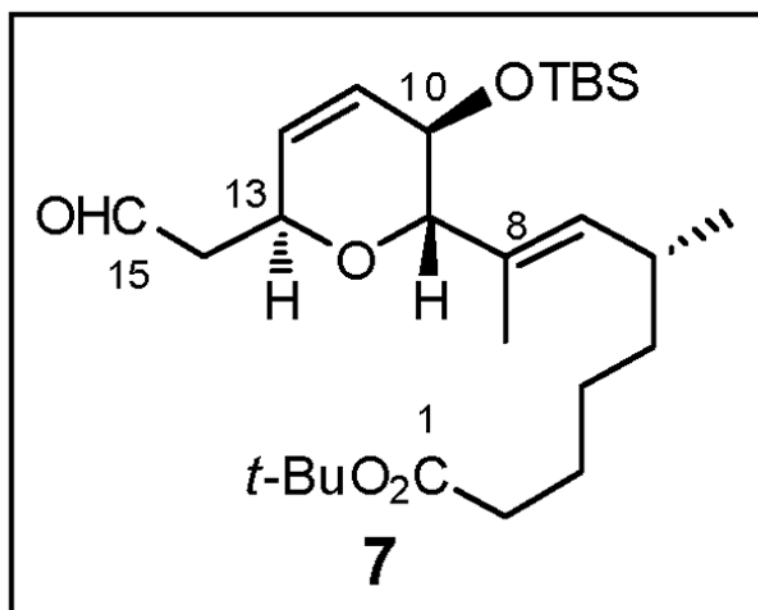


Fig 5.
Structure of DHP Fragment 7

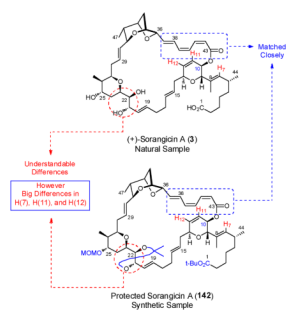


Fig 6.
Comparison of the ^1H NMR data for natural **3** and synthetic **142**

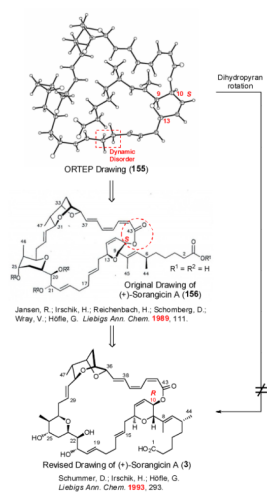


Fig 7.
Comparison of ORTEP of (+)-sorangicin A with two reported structures

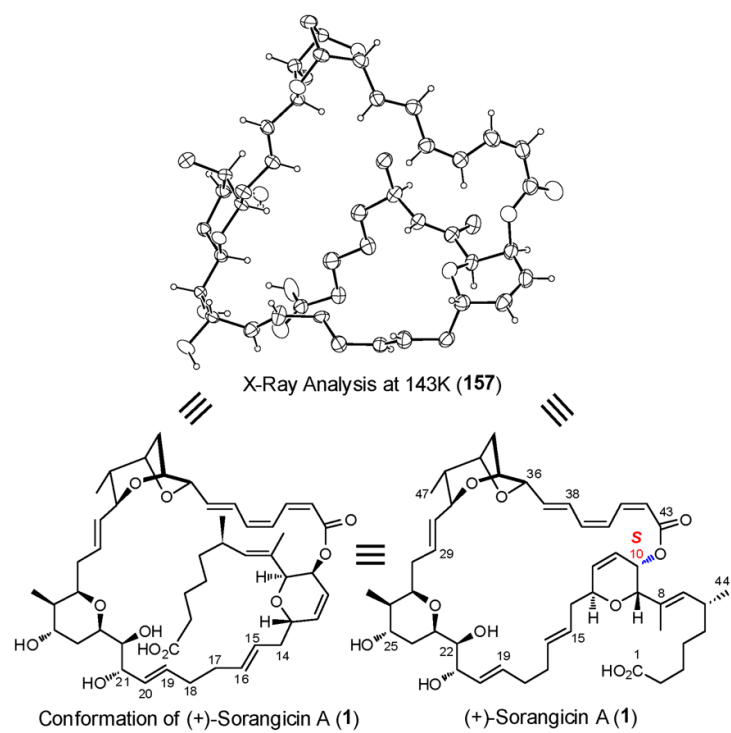
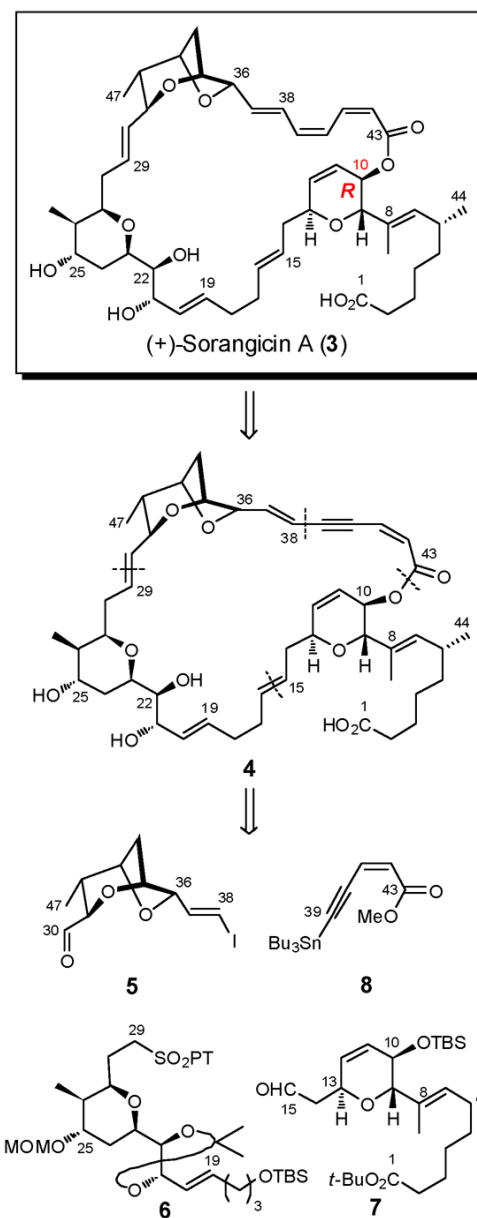
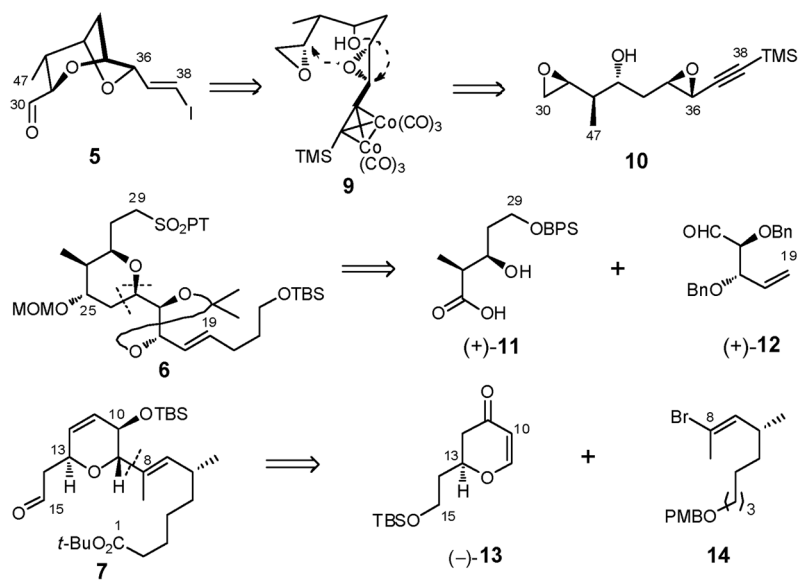


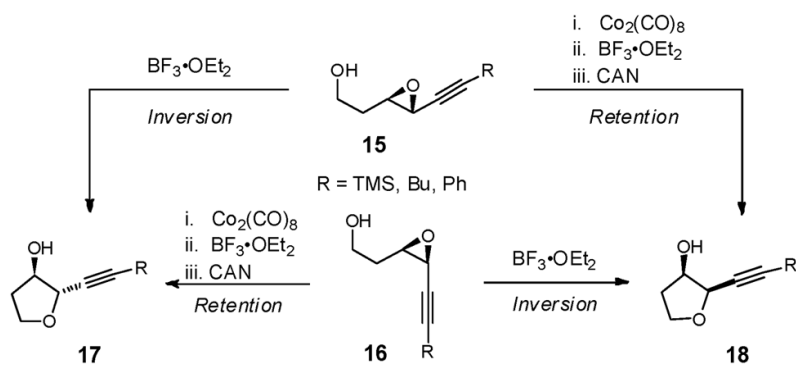
Fig 8.
X-ray structure verification of (+)-sorangicin A



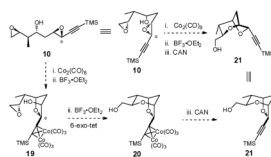
Scheme 1.



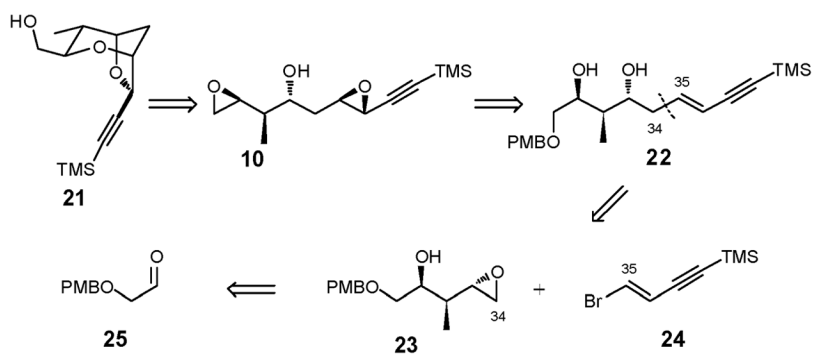
Scheme 2.



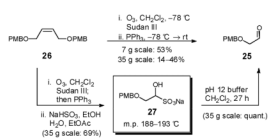
Scheme 3.



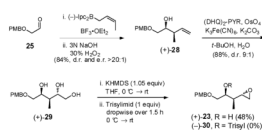
Scheme 4.



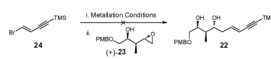
Scheme 5.

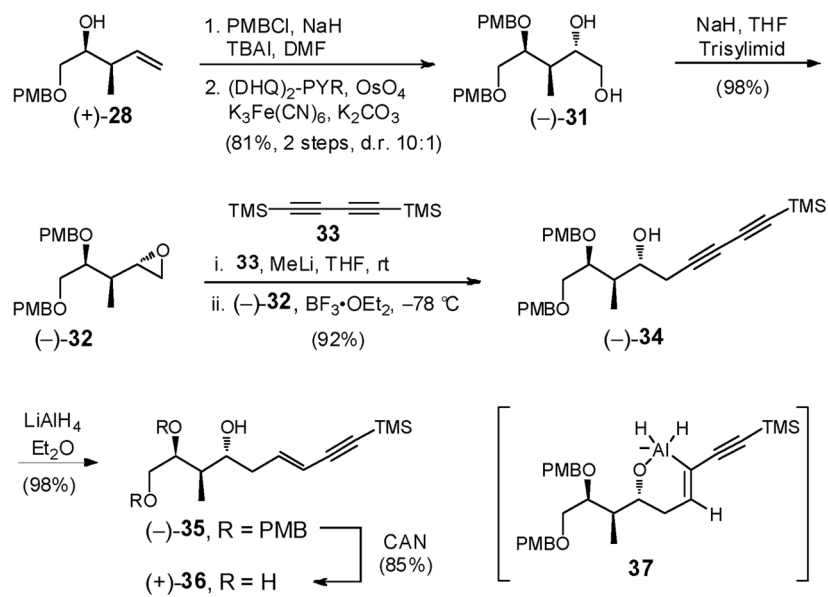


Scheme 6.

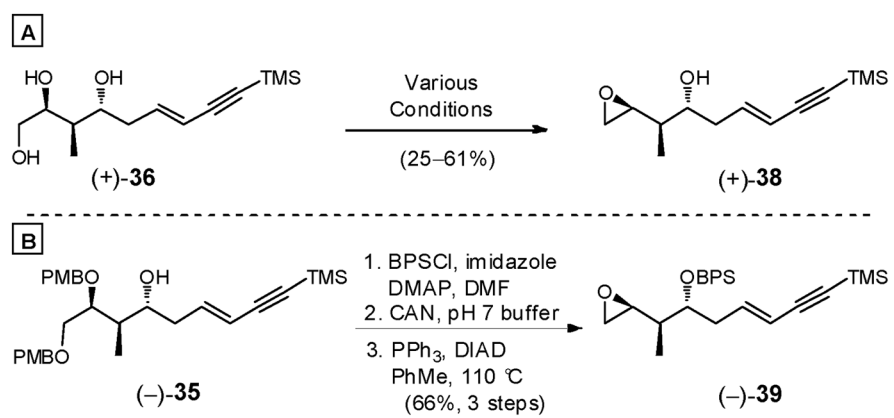


Scheme 7.

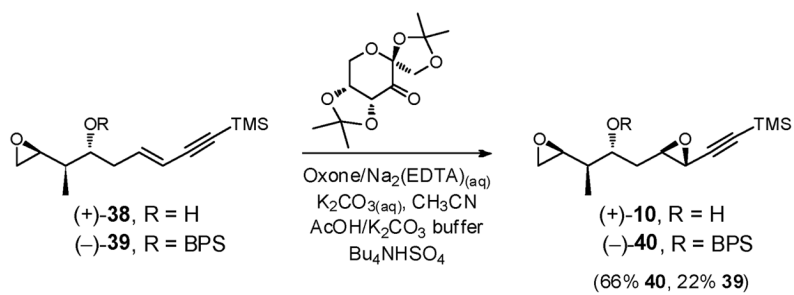
**Scheme 8.**



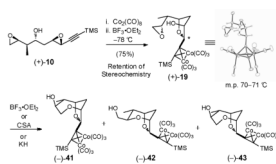
Scheme 9.



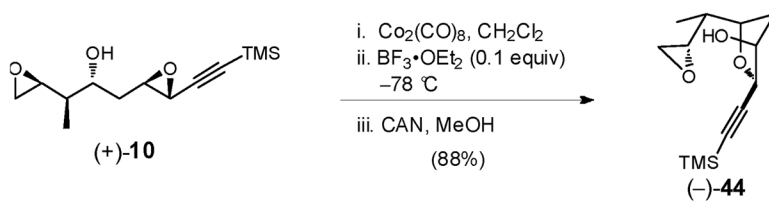
Scheme 10.



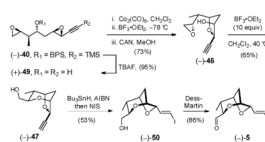
Scheme 11.



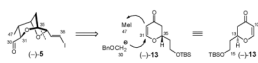
Scheme 12.

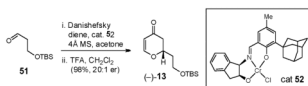


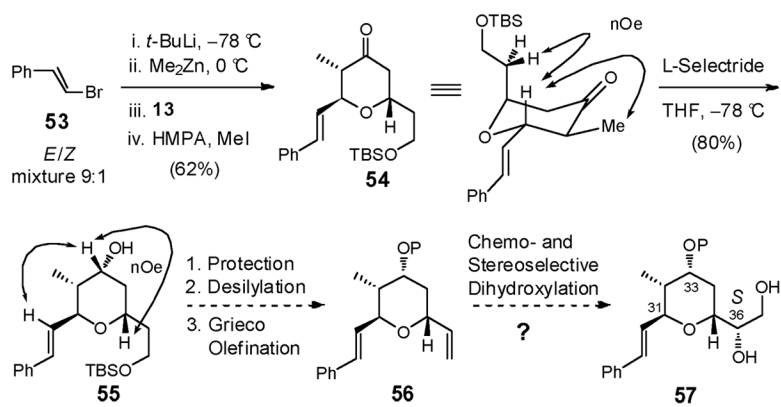
Scheme 13.



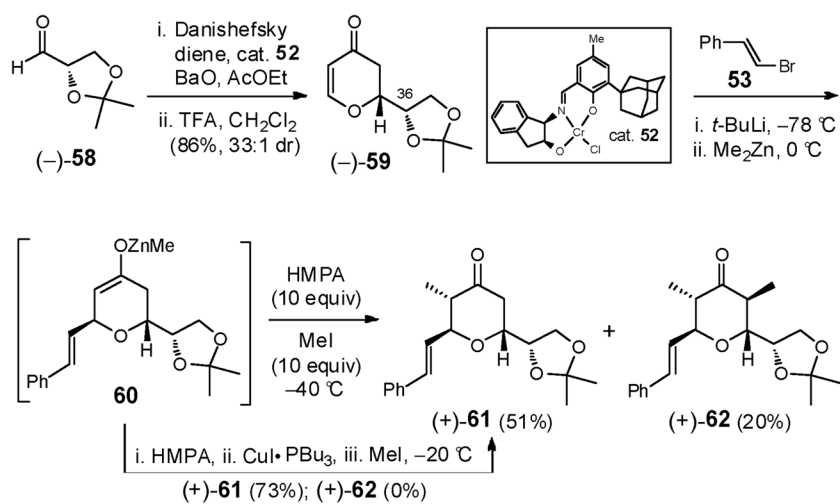
Scheme 14.

**Scheme 15.**

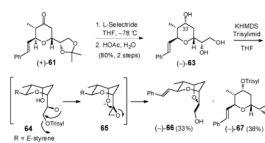
**Scheme 16.**



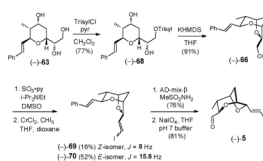
Scheme 17.



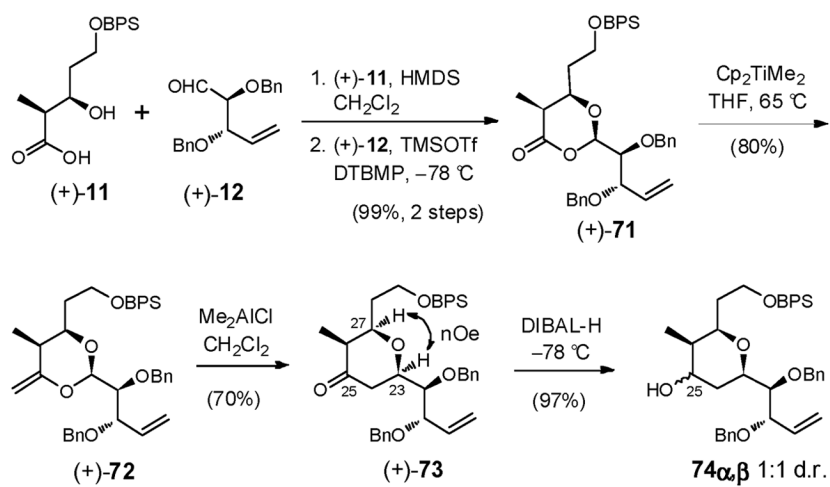
Scheme 18.



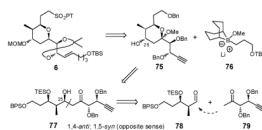
Scheme 19.



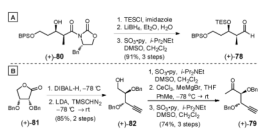
Scheme 20.



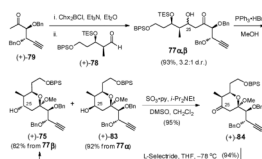
Scheme 21.



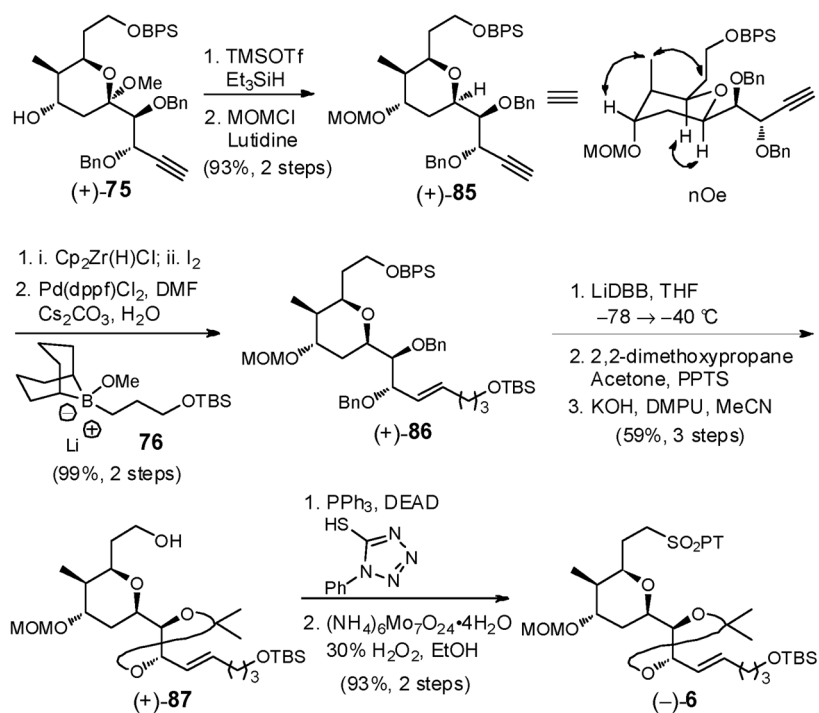
Scheme 22.



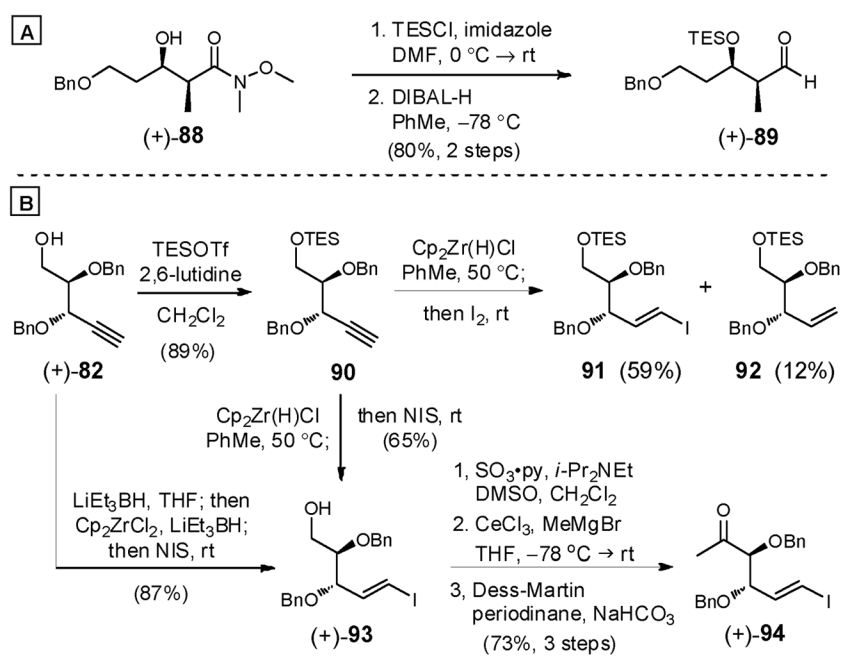
Scheme 23.



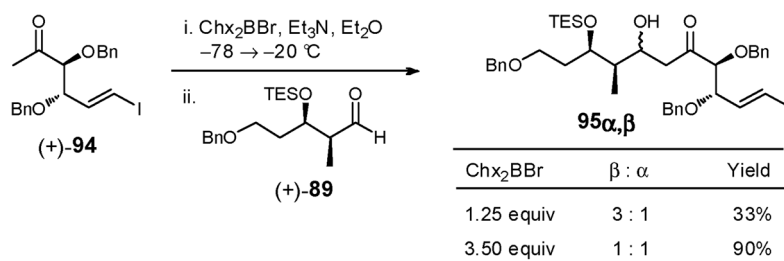
Scheme 24.



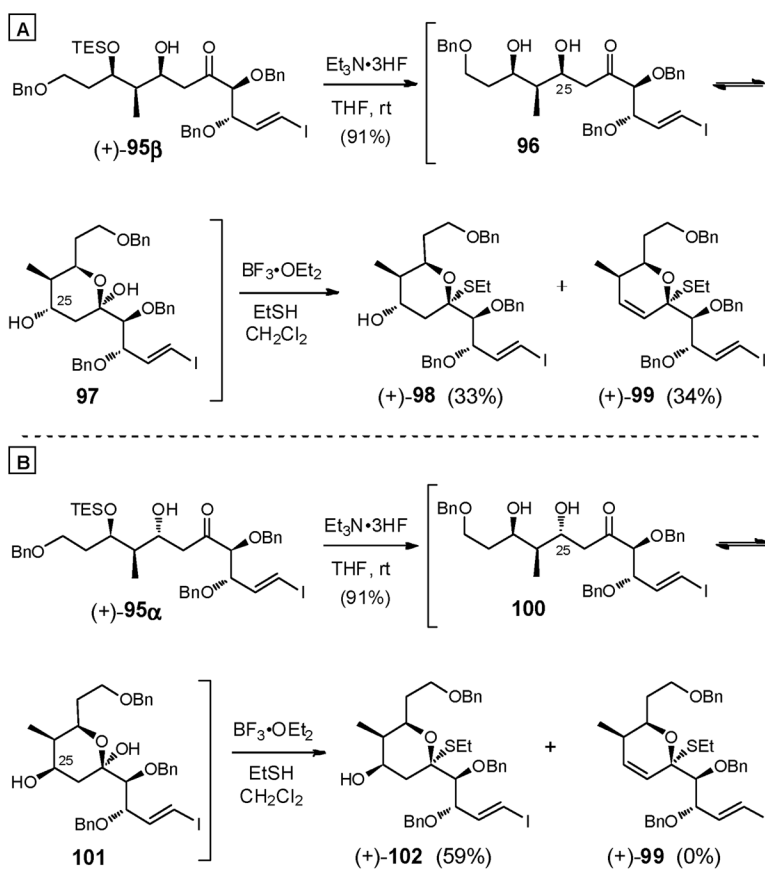
Scheme 25.



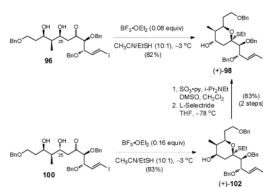
Scheme 26.



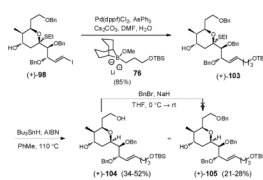
Scheme 27.



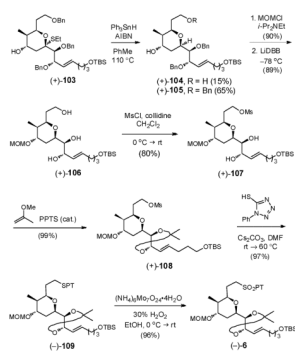
Scheme 28.



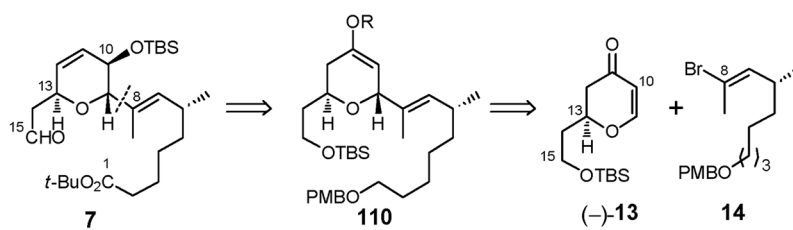
Scheme 29.



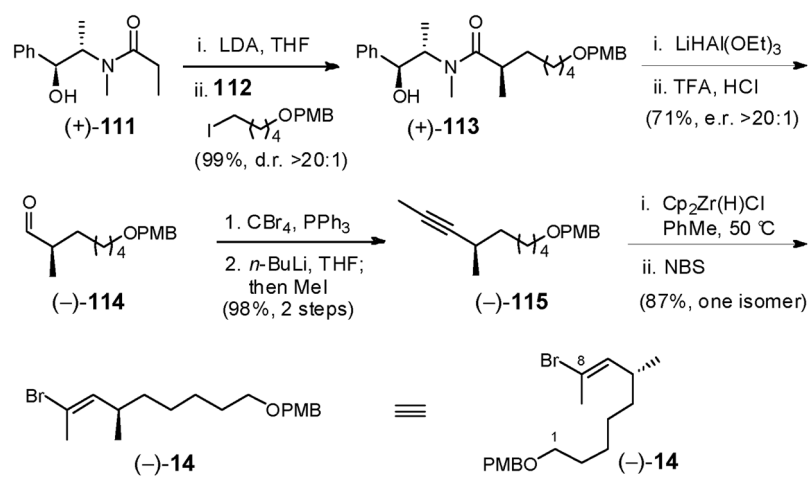
Scheme 30.



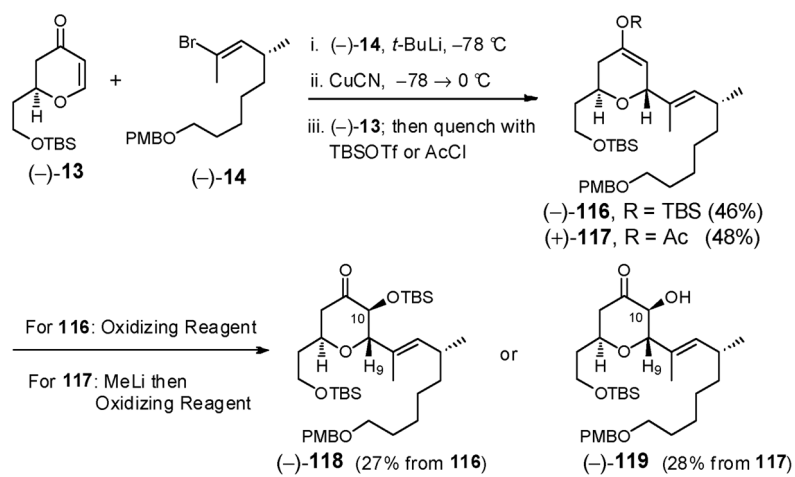
Scheme 31.



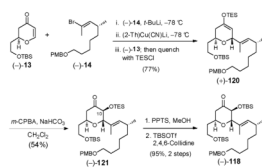
Scheme 32.



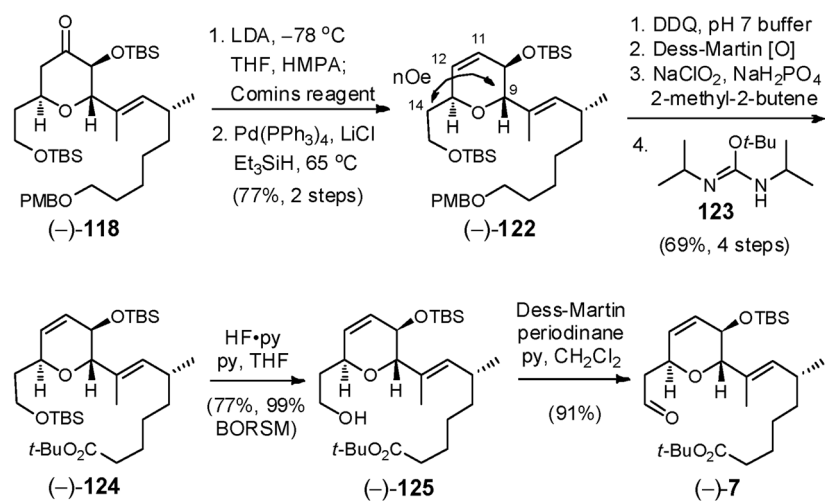
Scheme 33.



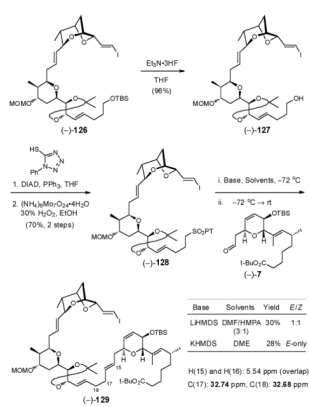
Scheme 34.



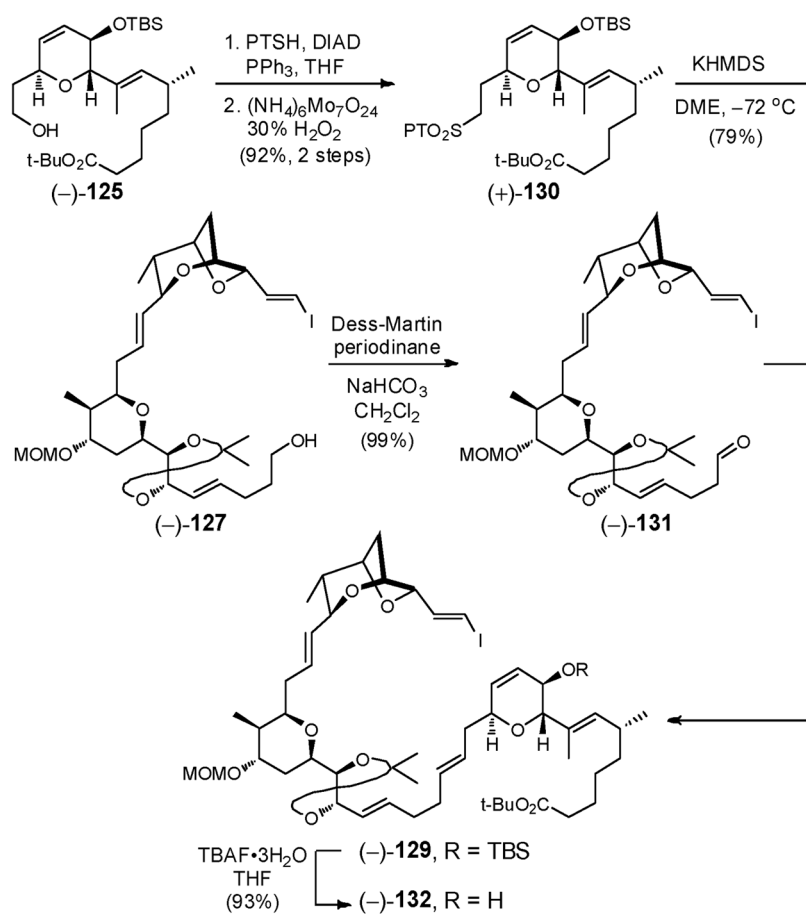
Scheme 35.



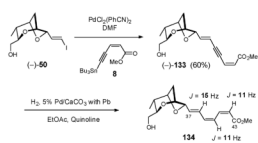
Scheme 36.



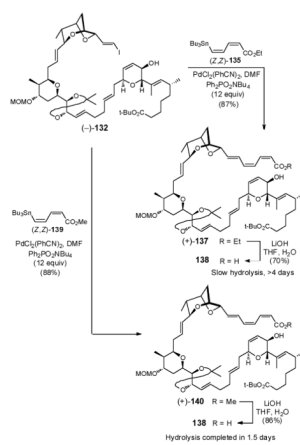
Scheme 37.



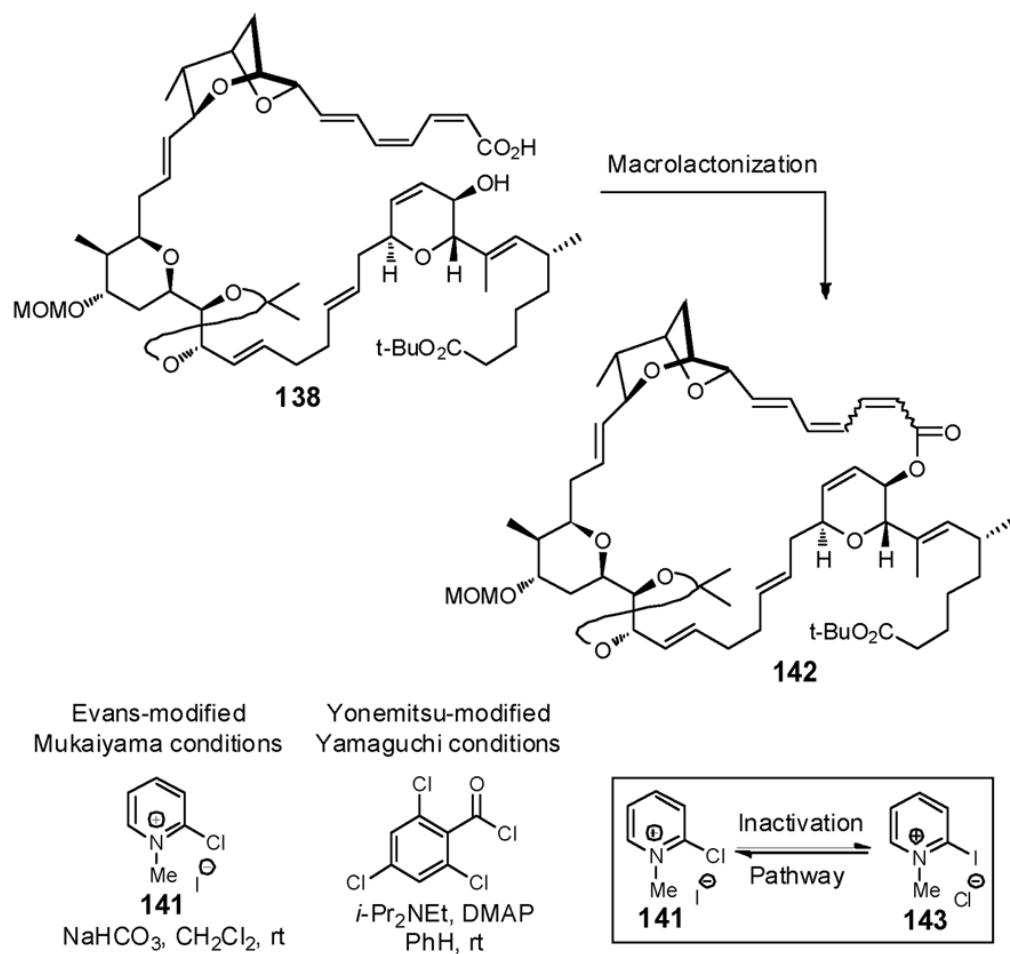
Scheme 38.



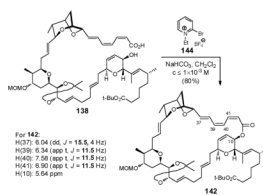
Scheme 39.



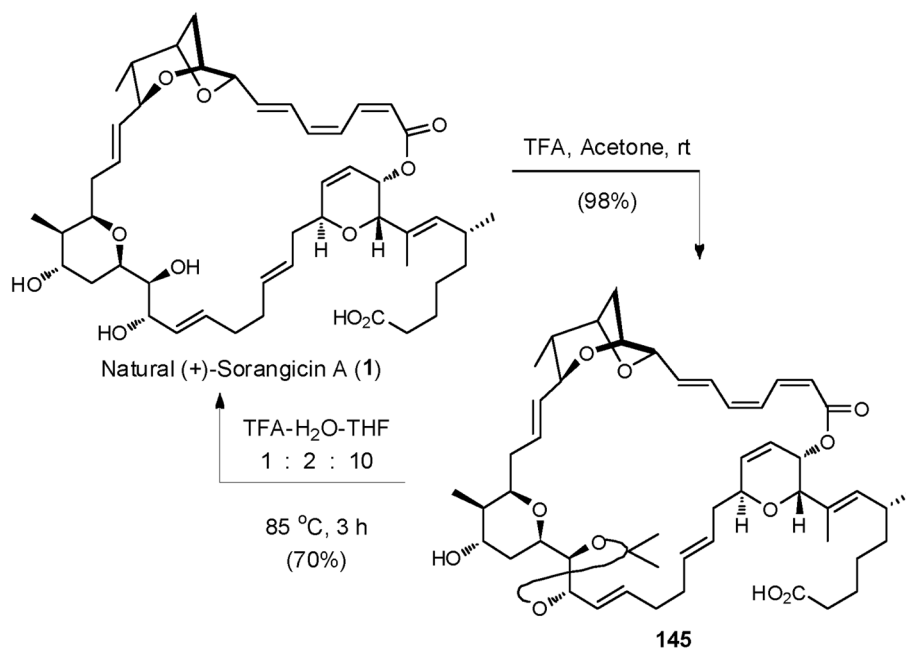
Scheme 40.



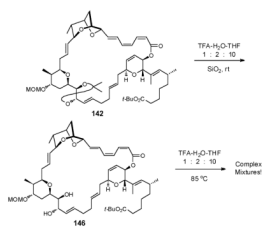
Scheme 41.

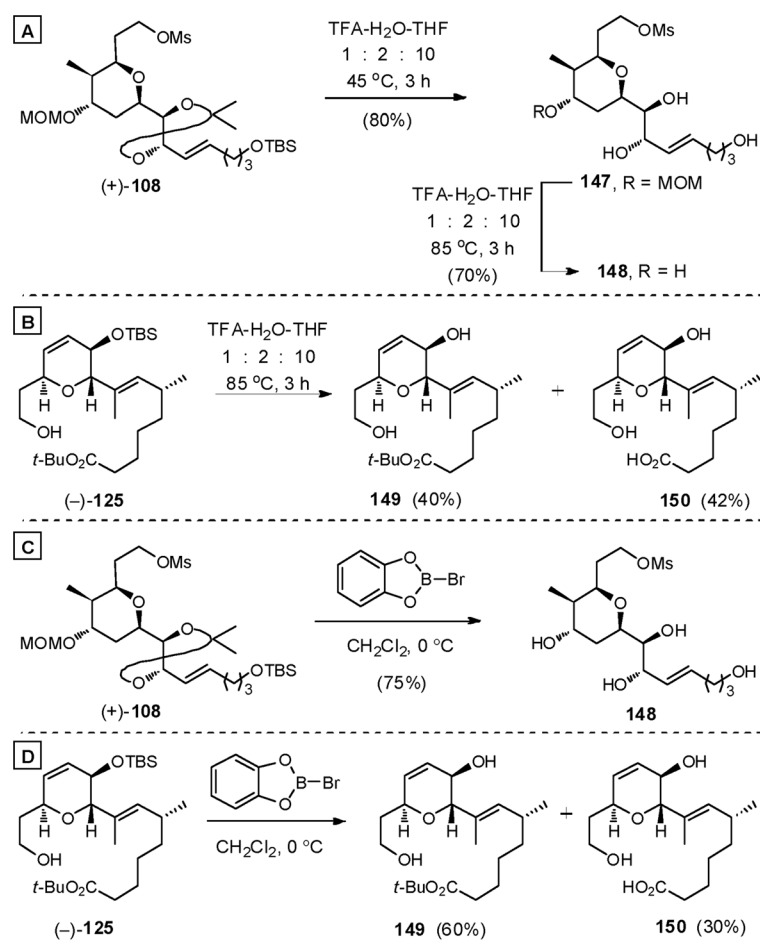


Scheme 42.

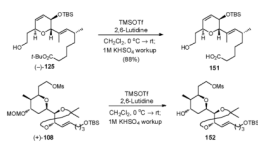


Scheme 43.

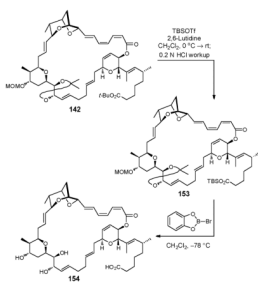
**Scheme 44.**



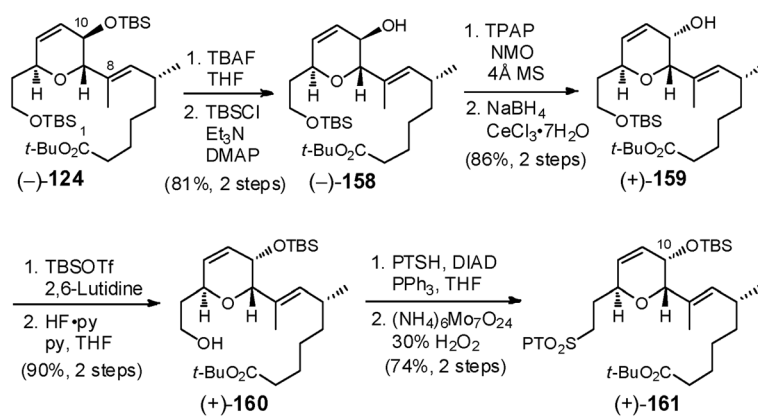
Scheme 45.



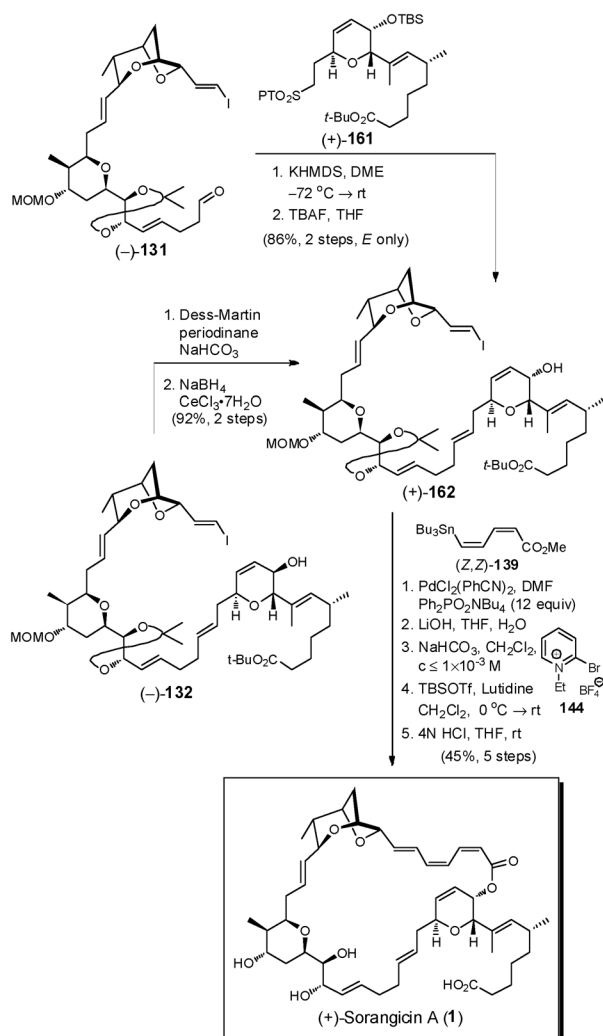
Scheme 46.



Scheme 47.



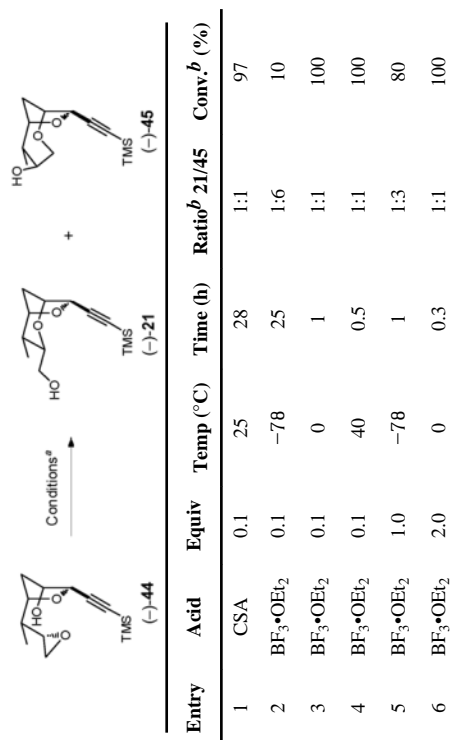
Scheme 48.



Scheme 49.

Table 1

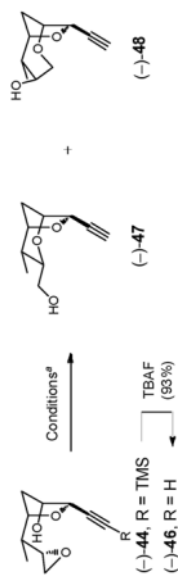
Cyclization of (-)-44



Entry	Acid	Equiv	Temp (°C)	Time (h)	Ratio ^b 21/45	Conv. ^b (%)
1	CSA	0.1	25	28	1:1	97
2	BF ₃ •OEt ₂	0.1	-78	25	1:6	10
3	BF ₃ •OEt ₂	0.1	0	1	1:1	100
4	BF ₃ •OEt ₂	0.1	40	0.5	1:1	100
5	BF ₃ •OEt ₂	1.0	-78	1	1:3	80
6	BF ₃ •OEt ₂	2.0	0	0.3	1:1	100

^a Entries 1–6 were run in CH₂Cl₂.^b Ratios and conversions were determined by ¹H NMR.

Table 2

Cyclization of (-)-**46**

Entry	Acid	Equiv	Temp (°C)	Time (min)	Ratio ^b 47/48	Conv. ^b (%)
1	BF ₃ •OEt ₂	0.1	0	60	1.4:1	100
2	BF ₃ •OEt ₂	10	40	5	2.1:1	100 ^c
3	TfOH	3.0	0	1	2.5:1	100
4	FSO ₃ H	0.1	0	5	2:1	100
5	SO ₃ H:SBF ₅ (1:1) ^d	NA	-20	5	> 2:1	100
6	None	NA	-20	weeks	1:2	NA

^a Entries 1–4 were run in CH₂Cl₂.

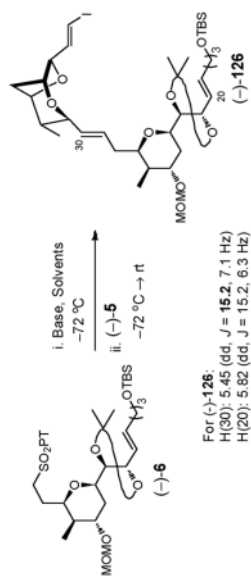
^b Ratios and conversions were determined by ¹H NMR.

^c Isolated yield for (-)-**47** was 65%.

^d Entry 5 was run in SO₂.

Table 3

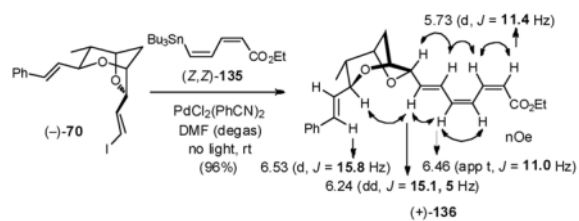
Olefination Conditions to Afford (-)-126



Entry	Base	Solvents	Yield	E/Z Ratio	Recov'd Sulfone	Recov'd Aldehyde
1	LiHMDS	DMF/HMPA (3:1)	24%	<i>E</i> -only	63%	36%
2	NaHMDS	DME/HMPA (3:1)	40%	3.6:1	39%	23%
3	KHMDS	DME	54%	2.0:1	0%	0%
4	LDA	DMF/HMPA (3:1)	11%	<i>E</i> -only	38%	42%
5	<i>t</i> -BuLi	DMF/HMPA (3:1)	39%	<i>E</i> -only	39%	13%

Table 4

Model Stille coupling to afford (+)-136



Entry	Additive	Geometric Isomers
1	---	mixture
2	$\text{Ph}_2\text{PO}_2\text{NBu}_4$ (1.5 equiv)	mixture
3	$\text{Ph}_2\text{PO}_2\text{NBu}_4$ (6 equiv)	pure <i>Z,Z,E</i> isomer